In Vivo Analysis of Cadherin Function in the Mouse Intestinal Epithelium: Essential Roles in Adhesion, Maintenance of Differentiation, and Regulation of Programmed Cell Death

Michelle L. Hermiston and Jeffrey I. Gordon

Department of Molecular Biology and Pharmacology, Washington University School of Medicine, St. Louis, Missouri 63110

Abstract. A model system is described for defining the physiologic functions of mammalian cadherins in vivo. 129/Sv embryonic stem (ES) cells, stably transfected with a dominant negative N-cadherin mutant (NCADΔ) under the control of a promoter that only functions in postmitotic enterocytes during their rapid, orderly, and continuous migration up small intestinal villi, were introduced into normal C57Bl/6 (B6) blastocysts. In adult B6↔129/Sv chimeric mice, each villus receives the cellular output of several surrounding monoclonal crypts. A polyclonal villus located at the boundary of 129/Sv- and B6-derived intestinal epithelium contains vertical coherent bands of NCADΔ-producing enterocytes plus adjacent bands of normal B6-derived enterocytes. A comparison of the biological properties of these cell populations established that NCADΔ disrupts cell–cell and cell–matrix contacts, increases the rate of migration of enterocytes along the crypt-villus axis, results in a loss of their differentiated polarized phenotype, and produces precocious entry into a death program. These data indicate that enterocytic cadherins are critical cell survival factors that actively maintain intestinal epithelial function in vivo.

THE cadherins are a superfamily of transmembrane glycoproteins that mediate homophilic, Ca^{2+}-dependent interactions between cells (Takeichi, 1991; Kemler, 1993). E- cadherin is the predominant cadherin found in epithelial cells. Studies in cultured cells suggest that E-cadherin may play a critical role in establishing and/or maintaining a differentiated phenotype. For example, disrupting E-cadherin-mediated adhesion can lead to dissociation of epithelial monolayers and dedifferentiation to a fibroblast-like morphology (Behrens et al., 1985; Gumbiner and Simons, 1986). Expression of E-cadherin in nonepithelial cell lines can produce an adherent, polarized, epithelial-like monolayer (Nagafuchi et al., 1987; McNeill et al., 1990). E-cadherin can induce assembly of adherens and other types of junctional complexes (Gumbiner et al., 1988; Jongen et al., 1991; Watabe et al., 1994), maintain the organization of the actin cytoskeleton (Frixen and Nagamine, 1993), promote a polarized distribution of organelles and cellular proteins (McNeill et al., 1990), and inhibit cell proliferation (Watabe et al., 1994). Downregulation of E-cadherin expression in transformed cell lines is associated with dedifferentiation and acquisition of the capacity to invade, suggesting that cadherins may function as tumor suppressors in vivo (Behrens et al., 1989; Frixen et al., 1991; Vleminckx et al., 1991).

Members of the cadherin family have distinct spatial and temporal patterns of expression during embryonic development and in the adult (for review see Takeichi, 1988; Ranscht, 1994). There have only been a limited number of reports describing the results of manipulating cadherin function in vivo. Expression of dominant-negative cadherin mutants in *Xenopus* embryos disrupts cell adhesion and tissue morphogenesis (Kinter, 1992; Levine et al., 1994; Dufour et al., 1994; Holt et al., 1994). Mouse embryos homozygous for an E-cadherin null allele are unable to form a trophoectodermal epithelium or a blastocyst cavity (Larue et al., 1994). Because of this early embryonic lethality, it has not been possible to define, in vivo, the physiologic functions of mammalian cadherins either during or after completion of organogenesis.

The mouse intestinal epithelium provides an attractive model for analyzing cadherin function because the entire developmental sequence of cell proliferation, lineage allocation, migration-associated differentiation, and programmed cell death can be surveyed at any moment in time along its crypt-villus axis. Perpetual cellular renewal is fueled by multipotent stem cells located near the base of each crypt of Lieberkühn (Loeffler et al., 1993). Studies of aggregation chimeras indicate that by the time intestinal morphogenesis is completed during the third postnatal week, each crypt is monoclonal, supplied by stem cells with identical genotypes,

Please address all correspondence to J. I. Gordon, Department of Molecular Biology and Pharmacology, Washington University School of Medicine, 660 South Euclid Avenue, St. Louis, MO 63110. Tel.: (314) 362-7243. Fax: (314) 362-7058.

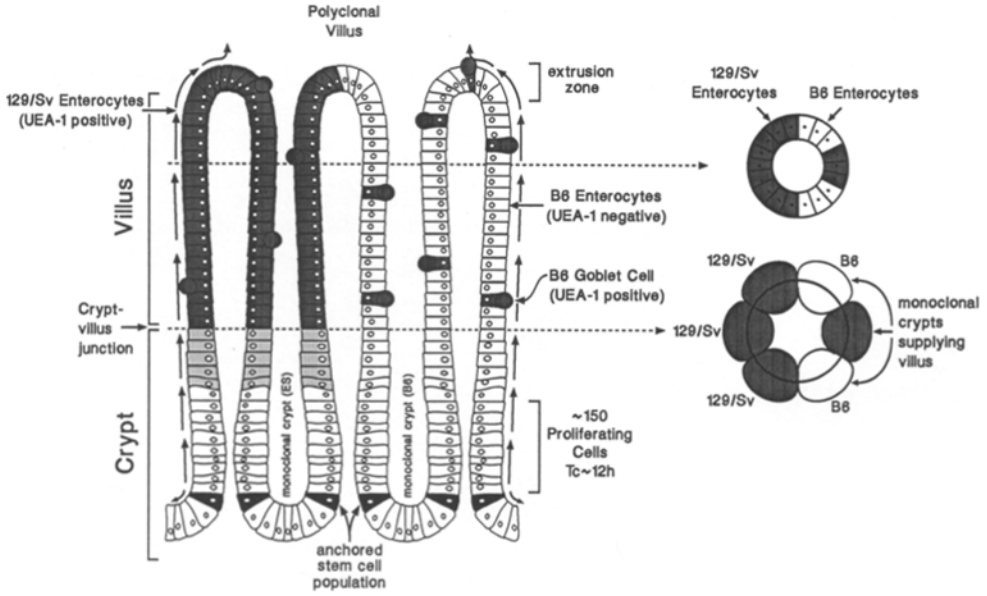

Figure 1. Schematic view of the small intestinal epithelium of an adult B6↔129/Sv chimeric mouse. A polyclonal villus located at the border of 129/Sv ES cell- and B6 blastocyst-derived epithelium has been sectioned parallel or perpendicular to the crypt-villus axis. A monoclonal crypt derived from stably transfected 129/Sv ES cells supplies a band of UEA-1–positive enterocytes to the villus. An adjacent monoclonal B6 crypt supplies a band of UEA-1–negative enterocytes to the same villus. Note that a subset of B6-derived goblet cells also bind UEA-1.

and each villus is polyclonal, supplied by several surrounding crypts (Schmidt et al., 1985, 1988). The stem cells' immediate descendants undergo rapid amplification in the middle third of the crypt and are allocated to one of the four principal epithelial lineages. Differentiation is completed during a bipolar migration. Defensin- and growth factor–producing Paneth cells migrate downward to the base of the crypt where they reside for ~20 d before being removed by phagocytosis (Cheng, 1974; Bry et al., 1994). Absorptive enterocytes, enteroendocrine, and mucus-producing goblet cells migrate upward in vertical coherent bands from each crypt to the apical extrusion zone of a surrounding villus (Schmidt et al., 1985). The sequence of proliferation in cell cycle arrest, migration-associated differentiation, followed by programmed cell death and extrusion from the villus tip is repeated every 3–5 d for these three lineages (Wright and Irwin, 1982; Gavrieli et al., 1992; Hall et al., 1994; for review see Hermiston et al., 1994). The stem cell hierarchy and functional organization of the intestine's crypt-villus units are ideally suited for creating chimeric-transgenic mouse models to study the effects of various gene products on epithelial cell biology (Hermiston et al., 1993). Embryonic stem (ES)[1] cells (129/Sv origin), stably transfected with a recombinant DNA consisting of an intestine-specific promoter linked to a gene encoding the protein of interest, are introduced into a normal C57Bl/6 (B6) blastocyst. A polyclonal villus positioned at the border of 129/Sv and B6 components of the chimeric mouse's small intestine will contain a discrete band of 129/Sv-derived enterocytes that express the transgene adjacent to a (control) band of normal B6-derived enterocytes (Fig. 1). The B6 and 129/Sv stripes can be distinguished by differences in their ability to bind the L-α-fucose-specific lectin *Ulex europeaus* agglutinin type 1 (UEA-1; Fig. 1; cf Hermiston et al., 1993). The power of the system lies in the ability to directly define the biological consequences of transgene expression by comparing adjacent bands of cells that share an identical microenvironment.

In this report, we have used chimeric-transgenic mice as an in vivo mammalian model to examine the function of cadherins. E- cadherin is the predominant cadherin in the intestinal epithelium, although distantly related family members are also detectable (Boller et al., 1985; Berndorff et al., 1994; Dantzig et al., 1994). Experiments in *Xenopus* embryos and a transfected mouse keratinocyte cell line have shown that an N-cadherin mutant lacking the extracellular domain (NCADΔ) can disrupt the functions of heterologous cadherins (Kinter, 1992; Fujimori and Takeichi, 1993). We expressed NCADΔ in enterocytes which account for >90% of the cells in the small intestinal epithelium (Cheng and Leblond, 1974). Expression was confined to villus-associated enterocytes so that we could study the contributions of cadherins to cell–cell and cell–matrix adhesion, to the regulation of cell migration rates and pathways, to the establishment and maintenance of a polarized differentiated state, and to the programming of cell death.

Materials and Methods

Construction of Transgenes

A 1.8-kb XhoI–KpnI DNA fragment, containing the neomycin resistance gene under the control of the phosphoglycerate kinase promoter (pgkNeo), was excised from pPNT (Tybulewicz et al., 1991) and subcloned into XhoI–KpnI-digested pBluescript I KS$^+$ (Stratagene, La Jolla, CA), yielding pPgkNeoBS. A 3.5-kb EcoRI fragment containing nucleotides −1178 to +28 of rat *Fabpi* linked to nucleotides +3 to +2150 of the human growth hormone gene (I-FABP$^{-1178\ to\ +28}$/hGH; Sweetser et al., 1988) was placed at the EcoRI site of pPgkNeoBS, generating pII178hGHpNeo with I-FABP$^{-1178\ to\ +28}$/hGH located upstream and in the same transcriptional orientation as the pgkNeo selection cassette.

The human growth hormone gene contains a BamHI site at its nucleotide +3. pII178hGHDon has two additional BamHI sites, one located 3′ to pgkNeo and the other in the pBluescript polylinker 5′ to I-FABP$^{-1178\ to\ +28}$/hGH. These two sites were eliminated by partial digestion of the plasmid

1. *Abbreviations used in this paper*: B6, normal C57Bl/6; BrdU, 5′-bromo-2′-deoxyuridine; ES, embryonic stem; GMA, *Glycine Max* agglutinin; hGH, human growth hormone; NCADΔ, N-cadherin mutant lacking the extracellular domain; PAP, peroxidase-anti-peroxidase; PAS, Periodic Acid Schiff; TdT, terminal deoxynucleotidyl transferase; TUNEL, dUTP nick end labeling; UEA-1, *Ulex europeaus* agglutinin type 1.

with BamHI, treatment with Klenow, ligation, followed by one more cycle of this process, yielding pI1178hGHpNeoB$_2$. pSP72NCADΔC (kindly provided by Chris Kinter) contains a dominant-negative *Xenopus* N-cadherin mutant cDNA (NCADΔC) with an in-frame deletion encompassing most of the extracellular domain of the mature protein. The signal peptide, transmembrane, and intracellular domains are retained (Kinter, 1992). NCADΔC cDNA was excised from pSP72NCADΔC with XhoI and EcoRV. The XhoI end was filled in with Klenow, BglII linkers were added, and the 1.2-kb fragment was ligated to BamHI-digested pI1178hGHpNeoΔB$_2$, yielding pI1178NCADΔChpNeo. (hGH will not be produced from the insert in this plasmid since the initiator Met codon and the first stop codon are from NCADΔC DNA and there is no ribosomal reentry site to reinitiate translation at the downstream initiator ATG of hGH.)

Culture and Electroporation of ES Cells

D3 ES cells (Doetschman, 1985) were used at passages 8–15 and maintained on Sto or mouse embryonic fibroblast feeder layers in ES media (Robertson, 1987). The inserts in pI1178hGHpNeoB$_2$ and pI1178NCADΔChpNeo were separated from vector sequences by digestion with XbaI, followed by electrophoresis through SeaPlaque low melting point agarose (Midwest Scientific, St. Louis, MO). DNA fragments were recovered from the gel using β-agarose (New England Biolabs, Beverly, MA). ES cells (2×10^7/0.5 ml PBS) were electroporated with 10 μg of the purified DNA fragments using a Gene Pulser (960 μf, 200 mV, 0.4-cm cuvette). Cells were plated at a density of $\sim 2 \times 10^6$ cells/60-mm feeder plate. G418 selection was begun 36 h after electroporation. 24 D3-I1178hGH colonies and 12 D3-I1178NCADΔ colonies were randomly selected from the 500–700 G418-resistant colonies obtained 10 d after transfection. They were expanded to a 48-well plate. After 2–3 d, confluent clones were harvested. Seventy five percent of the cells were passaged to a 35-mm dish, grown to near-confluence, trypsinized, and frozen in freezing mix (10% DMSO, 40% FCS, and 50% ES cell media). The remaining cells were cultured for 4–5 d in gelatinized 24-well plates for subsequent isolation of genomic DNA.

Characterization of D3-I1178hGH and D3-I1178NCADΔ ES Cell Lines

Mouse intestinal fatty acid–binding protein is not detectable by Western blot analysis of lysates prepared from D3 ES cells maintained on Sto cells (Green, R., and J. Gordon, unpublished data). To determine if I-FABP$^{-1178 \text{ to } +28}$ is silent in ES cells, medium harvested from each of the 24 confluent D3-I1178hGH cell lines were assayed in duplicate for the presence of hGH with a sensitive radioimmunoassay (Nichols Institute, San Juan Capistrano, CA). This radioimmunoassay does not recognize mouse or bovine growth hormone and can detect as little as 1 ng hGH/mL. No hGH was found in any of the samples.

Genomic DNA was purified from each stably transfected ES cell line and screened for the presence of hGH genomic sequences by PCR. Oligonucleotide primers to the antisense strand of exon 1 (5′-AGGTGGCCTTTGACACCTACCAGG-3′) and to the sense strand of exon 3 (5′-TCTGTTGTGTTTCCTCCCTGTTGG-3′) were used to amplify a 360-bp hGH fragment. The PCR mixture (final volume = 20 μl) contained 50 mM KCl, 10 mM Tris (pH 8.4), 2 mM $MgCl_2$, 2 mg/ml gelatin, 200 μm dNTPs, 10 μM of each primer, 0.7 U Amplitaq (Perkin Elmer/Cetus, Norwalk, CT), and 1 μg genomic DNA. The following cycling conditions were used: denaturation = 1 min at 94°, annealing = 1 min 30 s at 55°, and extension = 2 min at 72° for a total of 25 cycles. All G418-resistant clones surveyed contained hGH DNA.

Production and Maintenance of Chimeric-Transgenic Mice

Moruli were harvested from superovulated, 3-wk-old B6 females that had been mated to B6 males. The moruli were cultured overnight at 37°C to the blastocyst stage under an atmosphere of 5% CO_2/95% air in Brinster's media (GIBCO BRL, Gaithersburg, MD) supplemented with penicillin and streptomycin. Two independent D3-I1178hGH cell lines were injected into the B6 blastocysts (10–20 ES cells/embryo) using standard methods (Bradley, 1987). Ten independent D3-I1178NCADΔ clones were injected (5–20 ES cells/embryo).

Animals were maintained in microisolator cages under a strictly controlled light cycle (lights on at 0600 h and off at 1800 h). Mice were given a standard chow diet (Ralston Purina No. 5010) and water *ad libitum*. A sentinel screening program as well as serological tests of blood obtained by cardiac puncture at time of sacrifice of each chimera verified that the chimeras were free of Hepatitis, Minute, Lymphocytic Choriomeningitis, Ectromella, Polyoma, Sendai, K, Pneumonia, and MAD viruses.

Lectin Staining of Wholemount Preparations of Small Intestine

6–8-wk-old male and female B6↔129/Sv, B6↔129/Sv-I1178hGH, or B6↔129/Sv-I1178NCADΔ chimeras (n = 2–4 animals/cell line) were sacrificed by cervical dislocation. Intestinal wholemounts, prepared as previously described (Hermiston et al., 1993), were incubated with peroxidase-conjugated *Ulex europaeus* agglutinin type 1 (UEA-I; Sigma Chem. Co., St. Louis, MO), diluted to a final concentration of 5 μg/ml with blocking buffer (Hermiston et al., 1993). Peroxidase activity was visualized using metal-enhanced 3′,3′-diaminobenzidine (DAB, Pierce Chemical, Rockford, IL).

Single and Multilabel Immunohistochemical Analyses

6–8-wk-old B6↔129/Sv, B6↔129/Sv-I1178hGH, and B6↔129/Sv-I1178NCADΔ male and female mice (n = 2–4 animals/ES cell line) were given an intraperitoneal injection of 5-bromo-2′-deoxyuridine (BrdU; Sigma; 120 mg/kg body weight) and 5-fluoro-2′-deoxyuridine (Sigma; 12 mg/kg) 60 h before sacrifice to label crypt cells in S-phase and monitor their subsequent migration along the crypt-villus axis. The entire gastrointestinal tract was removed en bloc immediately after sacrifice, flushed with ice-cold PBS, fixed in Bouin's solution for 6–12 h, and then washed with 70% ethanol. The small intestine was divided into equal thirds (designated duodenum, jejunum, and ileum). Each segment was opened with an incision along its cephalocaudal axis, and then rolled up from its proximal to distal end. Each of the resulting Swiss rolls (Griffith et al., 1988) was cut in half, parallel to the cephalocaudal axis, placed in a tissue cassette with the cut edge on one-half facing down and the cut edge of the other half facing up, embedded in paraffin, and forty, 5-μm thick serial sections were cut. Every fifth section was stained with hematoxylin and eosin to define cellular morphology and crypt-villus architecture. Bouin's fixed samples of liver, kidney, spleen, stomach, colon, lung, heart, pancreas, skeletal muscle, skin, gonads, and brain, isolated from B6↔I1178hGH D3 chimeras, were analyzed for the presence of immunoreactive hGH (see below). Small intestines from two mice/cell line were fixed in 10% phosphate buffered formalin and processed in the same fashion.

The methods used for single and multilabel immunocytochemical staining of paraffin-embedded sections are described in several publications (Roth et al., 1990; Hermiston et al., 1992; Falk et al., 1994). Briefly, sections were deparaffinized, and then rehydrated in PBS. Endogenous peroxidase activity was blocked by incubation in 1% H_2O_2/PBS if peroxidase-anti-peroxidase (PAP) development methods were used. An enzymatic unmasking step was included to visualize some antigen-antibody or lectin-glycoconjugate complexes. This entailed incubation of sections for 15 min at 37° in a solution containing 1 mg/ml chymotrypsin (prepared in 7 mM $CaCl_2$, pH 7.8). Sections were then placed in PBS-blocking buffer (BSA [1%, wt/vol], powdered skim milk [0.2%; omitted for lectin staining], Triton X-100 [0.3%]) for 15 min at room temperature followed by overnight incubation at 4°C with primary antisera or lectins (diluted in PBS-blocking buffer). Antigen-antibody complexes were visualized using (*a*) gold-labeled secondary antibodies with silver enhancement (IGSS; Amersham Corp., Arlington Heights, IL), (*b*) Cy3-labeled donkey anti-goat, rabbit, or rat secondary antibodies (Ig, diluted 1:500 in PBS-blocking buffer; Jackson Immunoresearch Labs, West Grove, PA); (*c*) Cy3-labeled sheep anti-digoxigenin (1:1,000; Falk et al., 1995*a*); (*d*) FITC-labeled donkey anti-rabbit Ig (1:100; Jackson Immunoresearch Labs); or (*e*) Cy3-labeled sheep anti-mouse Ig (1:200; Sigma). Biotinylated lectins were visualized with FITC-conjugated Extra-avidin (1:100; Sigma). Slides were washed in PBS and mounted in PBS/glycerol (1:1 vol/vol) or counterstained with hematoxylin, dehydrated, and mounted in Permount (Fischer).

The following antisera were used to stain Bouin's fixed tissues: rabbit anti-hGH (final dilution = 1:2,000; DAKO), goat anti-BrdU (1:3,000; Cohn and Lieberman, 1984), mouse anti-β-actin (1:1,000; Sigma), rabbit anti-rat liver fatty acid–binding protein (specificity = villus-associated enterocytes; final dilution = 1:1,000, Sweetser et al., 1988), rabbit anti-pan-cadherin (1:2,000; Sigma), rabbit anti-laminin (1:1,000, Sigma), rabbit anti-collagen IV (1:1,000, Collaborative Biomedical Products, Bedford, MA), and rabbit anti-heparin sulfate proteoglycan (1:200, Chemicon, Temecula, CA). A rat anti-E-cadherin monoclonal antibody (1:400; kindly provided by Rolf Kelmer, Max Planck Institute; Vestweber and Kemler, 1985) was used on

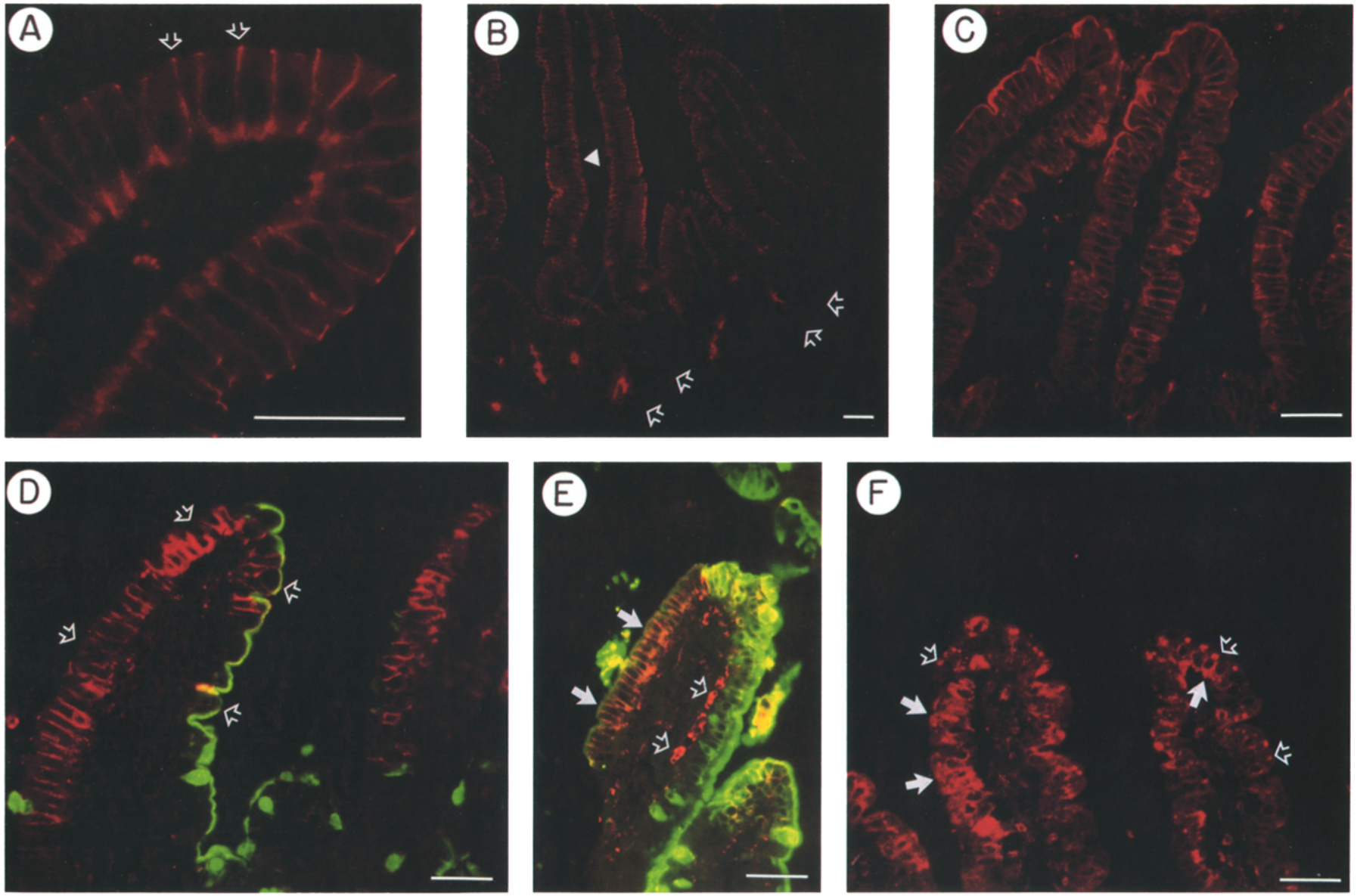

Figure 2. Immunocytochemical analysis of cadherin accumulation along the crypt-villus axis in adult B6↔129/Sv and B6↔129/Sv-I1178NCADΔ chimeras. (*A–C*) Sections from the proximal ileum of a normal B6↔129/Sv mouse (coat color chimerism = 95% 129/Sv). (*A*) Apex of a villus stained with a rat E-cadherin mAb (visualized with indocarbocyanine [Cy3]-conjugated donkey anti-rat Ig). The open arrows point to the apical junctional complexes. Note that immunoreactive protein is present throughout the lateral and basilar surfaces of enterocytes but is not detectable in their cytoplasm. (*B*) Lower power view of the entire crypt-villus axis. The section was treated as in *A*. Arrows point to the basolateral surfaces of crypt epithelial cells

formalin-fixed tissues. Control experiments demonstrated that none of the secondary antibodies labeled tissue sections in the presence of preimmune sera or in the absence of primary antisera.

The following five lectins were employed, all at a final concentration of 5 μg/ml: peroxidase-or biotin-conjugated UEA-1 (Sigma; carbohydrate specificity = Fucα1,2Galβ), peroxidase-conjugated *Dolichos biflorus* agglutinin (Sigma; GalNAcα-), peroxidase-conjugated *Helix pomentia* agglutinin (Sigma, α-GalNAc/GalNAcβ4Gal-) and peroxidase-conjugated Jacalin (*Artrocarpus integrifolis* agglutinin, EY-Labs [San Mateo, CA], Galα6Gal; Galβ3GalNAc), and peroxidase-conjugated soybean (*Glycine max*) agglutinin (Sigma, GalNAcα3GalNAc; GalNAcα/β3/4Gal). *Molucella laevis* lectin recognizes GalNAcα-glycoconjugates including the Tn antigen (GalNAcα1-*O*-Ser/Thr) and its sialylated counterpart, sialyl-Tn (NeuAcα2,6GalNAcα1-*O*-Ser/Thr), core structures for mucus glycoproteins known to be exposed under conditions where normal glycosylation pathways are disrupted (Itzkowitz et al., 1989). The lineage-specific, diffferentiation-dependent, and cephalocaudal patterns of reactivity of these lectins with the gut epithelium are documented in Hermiston et al. (1993) and in Falk et al. (1994, 1995*a*).

Periodic Acid Schiff (PAS), Alcian blue, and Gram stains were performed using standard methods. Terminal deoxynucleotidyl transferase (TdT)-mediated, dUTP nick end-labeling (TUNEL) assays were performed on formalin-fixed tissues exactly as described in Gavrieli et al. (1992).

Results

E-cadherin Expression in Normal B6↔129/Sv Mouse Intestine

The distributions of mouse E-cadherin along the crypt-villus and duodenal-colonic axes have not been reported. Therefore, sections of small intestine were prepared from 6–8-wk-old B6↔129/Sv mice that had been produced with nontransfected D3 ES cells (n = 5 animals; ≥95% 129/Sv contribution to coat color). Incubation of the sections with an E-cadherin monoclonal antibody (Vestweber and Kemler, 1985) revealed intense punctate staining at apical junctional complexes (Fig. 2, *A* and *B*; cf Boller et al., 1985). Weaker staining occurs along the lateral surfaces of epithelial cells. Basilar surface staining is also apparent while cytoplasmic staining is absent. A pan-cadherin antisera that recognizes a conserved epitope found at the COOH-terminal cytoplasmic tails of all known "classical" cadherins (Geiger et al., 1990; Kemler, 1992) gave similar results (Fig. 2 *C*). Both antisera disclosed that cadherins were associated with the apical rather than basolateral surfaces of crypt epithelial cells (Fig. 2 *B*). The intensity of staining increases at sites of cell–cell contact as enterocytes approach the villus' apical extrusion zone (Fig. 2, *B* and *C*). This distribution of E-cadherin along the crypt-villus axis parallels the proliferation of junctional complexes which occurs as enterocytes approach the villus tip (Madara, 1990).

Enterocytic levels of E-cadherin are equivalent in crypt-villus units located in the duodenum, jejunum, or ileum (data not shown). Multi-label studies with UEA-1 and the E-cadherin mAb revealed that 129/Sv- and B6-enterocytes located at a given cell stratum of a polyclonal villus have similar intracellular concentrations and distributions of E-cadherin (data not shown).

Nucleotides −1178 to +28 of the Rat Intestinal Fatty Acid–binding Protein Gene Can Deliver Foreign Gene Products to Villus-associated Enterocytes in B6↔129/Sv Mice

Nucleotides −1178 to +28 of the rat intestinal fatty acid–binding protein gene (I-FABP$^{-1178\ to\ +28}$) have been used to express a variety of gene products in the small intestinal epithelium of transgenic mice (Cohn et al., 1992; Kim et al., 1993; Simonet et al., 1994; Zhou et al., 1994). I-FABP$^{-1178\ to\ +28}$ is activated on embryonic day 15, coincident with initial cytodifferentiation of the pseudostratified intestinal endoderm to an epithelial monolayer overlying nascent villi. Expression is sustained at least through the first 18–24 mo of postnatal life (Kim et al., 1993). Reporter synthesis is confined to enterocytes, is only initiated as these cells exit the crypt, and is maintained until they are exfoliated at the villus tip (Cohn et al., 1992). Regional variations in I-FABP$^{-1178\ to\ +28}$/reporter expression are established and maintained along the duodenal-ileal axis with highest steady state levels occurring in the distal jejunum and proximal ileum (e.g., Cohn et al., 1992; Kim et al., 1993).

To assure ourselves that the expression domain of I-FABP$^{-1178\ to\ +28}$ is not affected by genetic background or by the pgkNeo selection cassette used to identify stably transfected ES cells, chimeric-transgenic mice were generated that contained this promoter linked to the human growth hormone (hGH) gene followed by pgkNeo. Wholemounts of small intestine, prepared from 6–8-wk-old B6↔129/Sv-I1178hGH mice, were stained with UEA-1 (n = 5 mice; 129/Sv coat color >80%). Highly chimeric areas (Fig. 3 *A*) were excised from the duodenum, jejunum, and ileum, and subjected to multi-label immunocytochemical analyses. The lineage-specific, differentiation-dependent, and cephalocaudal patterns of hGH accumulation were comparable to those obtained in multiple pedigrees of I1178hGH mice produced by pronuclear injection: i.e., hGH is confined to ES-derived, villus-associated enterocytes and absent from crypts (Fig. 3 *B*).

where E-cadherin is not detectable, in contrast to villus-associated enterocytes. (*C*) The section was incubated with a rabbit pan-cadherin antisera and antigen-antibody complexes were visualized with Cy3-conjugated donkey anti-rabbit Ig. The cellular levels and distributions of cellular cadherins are similar to what is observed with the E-cadherin mAb. (*D–F*) The intracellular level and distribution of cadherins are perturbed in villus-associated, 129/Sv-I178NCADΔ enterocytes. (*D*) Double exposure of a section of B6↔129/Sv-I1178NCADΔ ileum incubated with rat E-cadherin mAb (visualized with Cy3- labeled donkey anti-rat Ig) and biotin-conjugated UEA-1 (visualized with FITC-conjugated extra-avidin). A comparison of E-cadherin immunoreactivity (*red*) in UEA-1-positive enterocytes (stained green at their apical brush border) and UEA-1–negative enterocytes located at various cell strata along the crypt-villus axis (*open arrows*) reveals that expression of NCADΔ is associated with marked reductions in cellular E-cadherin levels. (*E*) Section of ileum stained as in *D*. The open arrows point to clumps of E-cadherin located at the basolateral surfaces of 129/Sv-I1178NCADΔ enterocytes. The pattern is quite distinct from that encountered in the adjacent band of UEA-1–negative B6 enterocytes (*closed arrows*). (*F*) Ileal villi containing a wholly 129/Sv-I1178NCADΔ-derived population of enterocytes were sectioned parallel to their crypt-villus axis. Sections were incubated with rabbit pan-cadherin antisera (visualized with Cy3-labeled donkey anti-rabbit Ig). As enterocytes migrate up these villi, there is a pronounced increase in steady state levels of immunoreactive cadherins at the surface of cells as well as throughout their cytoplasm (e.g., *closed arrows*). The open arrows highlight examples of cadherin aggregates that appear near the apex of enterocytes. Bars, 25 μm.

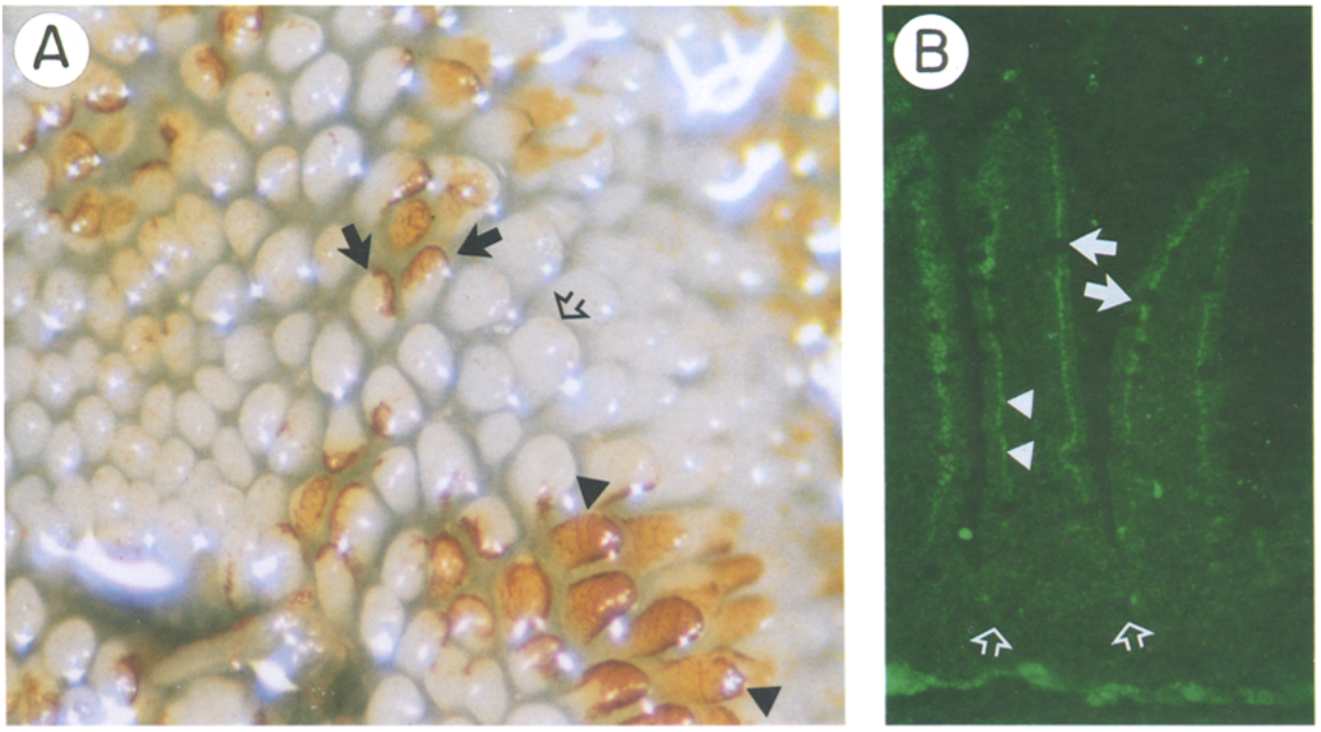

Figure 3. Immunocytochemical analysis of B6↔129/Sv-I1178hGH mice. (*A*) Wholemount of the distal third of the intestine incubated with peroxidase-conjugated UEA-1 (visualized with 3′,3′-diaminobenzidene). Clusters of wholly UEA-1–negative B6-derived villi (e.g., *open arrow*), wholly UEA-1–positive 129/Sv-I1178hGH-derived villi (*closed arrowheads*), and striped polyclonal supplied by both monoclonal B6- and monoclonal 129/Sv-I1178hGH crypts (*closed arrows*) are present. (*B*) A portion of the wholemount preparation shown in *A*, containing wholly UEA-1–positive villi, was embedded in paraffin and sectioned parallel to the crypt-villus axis. The sections were incubated with rabbit anti-hGH sera followed by gold-labeled goat anti–rabbit Ig and viewed with reflected light polarization microscopy. hGH is present in Golgi apparatus of villus-associated enterocytes (*closed arrowheads*). No immunoreactive protein is detectable in villus-associated goblet cells (*closed arrows*) or in the crypts (*open arrows*).

The Phenotype Produced by Expressing NCADΔ in Villus-associated Enterocytes

Evidence That High Percentage B6↔129/Sv-I1178NCADΔ Chimeras Are Not Viable. I-FABP$^{-1178\ to\ +28}$ was used to direct expression of the *Xenopus* dominant-negative N-cadherin mutant (Kinter, 1992). We initially injected six independent, cloned 129/Sv-I1178NCADΔ cell lines into B6 blastocysts (15–20 ES cells/blastocyst). Birthrates were low: only 28% of injected blasts produced live-born mice. Only 20% of the liveborn animals were chimeric as judged by their coat color (129/Sv contribution <40%). Cesarean section of late gestation recipient mothers revealed evidence of multiple resorbed fetuses. In contrast, injection of the nontransfected parental D3 ES cell line (or I1178hGH ES cells) resulted in threefold higher birth rates with >60% of these mice having >80% 129/Sv contribution to coat color. By reducing the number of ES cells injected/blastocyst to 5–10, we were able to produce B6↔129/Sv-I1178NCADΔ mice from eight independent cell lines. All these animals appeared healthy and their weights at 6–8 wk were similar to those of comparably aged, comparably chimeric B6↔129/Sv mice.

Analysis of Wholemount Preparations of B6↔129/Sv-I1178NCADΔ Intestine. UEA-1 staining of wholemount preparations of small intestine from 6–8-wk-old normal B6↔129/Sv mice revealed coherent columns of 129/Sv enterocytes extending from the crypt-villus junction to the apical extrusion zone of a polyclonal villus (Fig. 4, *A* and *B*). In 6–8-wk-old B6↔129/Sv-I1178NCADΔ mice, UEA-1–positive 129/Sv-I1178NCADΔ enterocytes appeared to have defects in adhesion and migration. There were gaps between UEA-1–positive enterocytes within a given column. There were also focal clusters of bulbous and deformed cells that

Figure 4. Wholemount preparation of ileum from a B6↔129/Sv-I1178NCADΔ mouse reveals abnormalities in epithelial cell adhesion and migration along the villus. (*A*) Wholemount of the distal third of the small intestine ("ileum") isolated from a normal 6-wk-old B6↔129/Sv mouse. The preparation was stained with peroxidase-conjugated UEA-1 (visualized with metal-enhanced DAB). Villus-associated, B6 enterocytes appear white while D3-derived enterocytes as well as a subset of B6 goblet cells appear brown. (*B*) Higher power magnification of a portion of the wholemount preparation shown in *A*. Enterocytes of a given genotype migrate in coherent, linear bands up polyclonal villi (*closed arrows*) to the apical extrusion zone at the midpoint of the villus tip. (*C*) High power view of wholemount preparation of ileum from a 6-wk-old B6↔129/Sv-I1178NCADΔ mouse, stained with UEA-1. UEA-1–positive (*brown*) I1178NCADΔ-enterocytes are not tightly adherent and do not migrate up the villus in linear coherent bands.

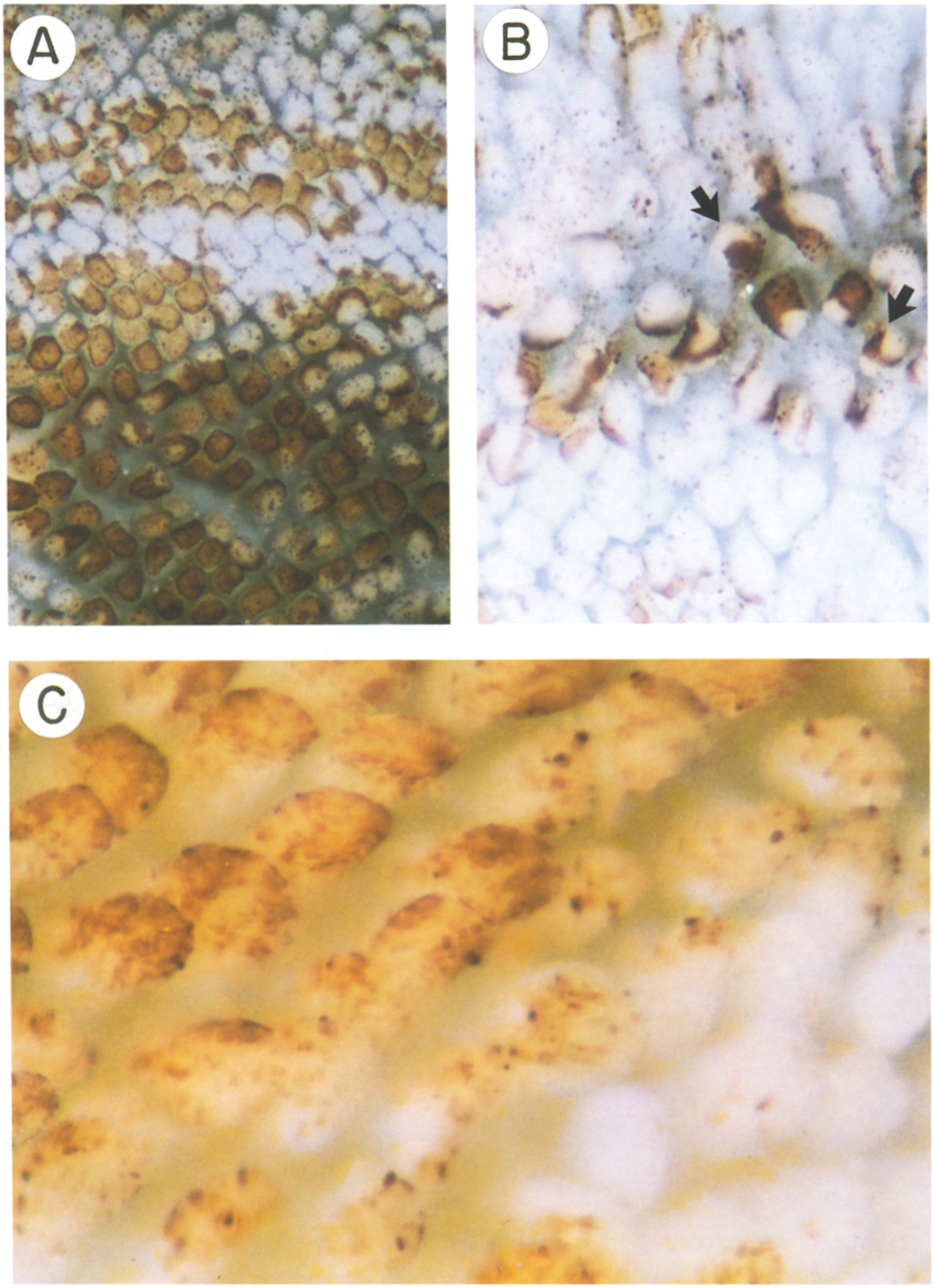
A
B
C

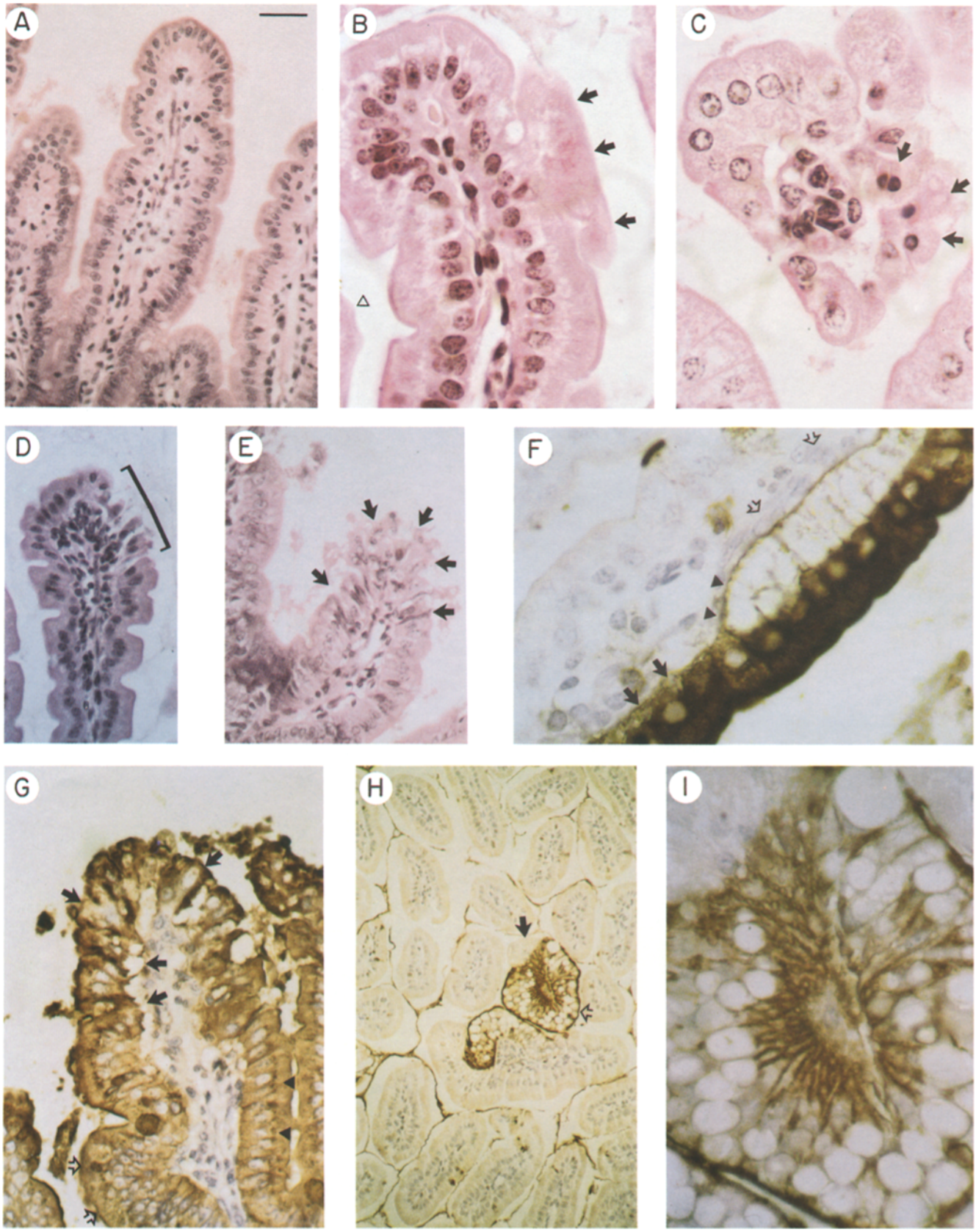

Figure 5. B6↔129/Sv-I1178NCADΔ mice display a variety of histologic abnormalities in their villus-associated epithelium. (*A*) Hematoxylin- and eosin-stained section of villi located in the proximal ileum of a normal B6↔129/Sv mouse (95% 129/Sv coat color). (*B–E*) Hematoxylin-and eosin-stained sections of small intestine from 6-wk-old B6↔129/Sv-I1178NCADΔ mice (30–50% 129/Sv coat color). (*B*) Arrows point to an outpouching of cells located near the tip of a jejunal villus. These cells lack a clearly defined apical brush

looked like blisters. The border between "columns" of UEA-1–positive and UEA-1–negative enterocytes was not well defined in polyclonal villi (Fig. 4 *C*). Nonetheless, the heights of wholly UEA-1–positive villi were similar to the heights of wholly UEA-1–negative villi.

These changes were evident in B6↔129/Sv-I1178NCADΔ mice produced from 5 of 8 independent ES cell lines (n = 3–5 mice analyzed/cell line; coat color chimerism = 20–50% for the progeny of the 5 cell lines compared to 40 to >95% for the 3 cell lines that yielded animals without a phenotype). The severity of the phenotypes observed in mice produced with each of the 5 cell lines varied along their duodenal-ileal axis. The most pronounced changes invariably occurred in the distal third of the small intestine (operationally defined as ileum). This regional variation parallels the known cephalocaudal pattern of I-FABP$^{-1178\ to\ +28}$/reporter expression.

A Range of Phenotypes Can be Ascribed to a 129/Sv-I1178NCADΔ Genotype. Sections were prepared from the entire duodenal-ileal axis of 6–8-wk-old B6↔129/Sv mice and comparably aged B6↔129/Sv-I1178NCADΔ chimeras (n = 2–4 mice from all 5 cell lines). Hematoxylin and eosin staining revealed that the morphology of enterocytes in normal B6↔129/Sv mice did not change appreciably from the crypt-villus junction to the apical extrusion zone. These cells have a uniform size, contain a homogeneously stained cytoplasm, possess a distinct apical brush border, and are tightly adherent to their neighbors (Fig. 5 *A*). Less than one in 750 villi show evidence of active cell extrusion (as defined by Madara, 1990). When detected, cells are extruded singly or in pairs from the villus tip. In contrast, hematoxylin- and eosin-stained sections of B6↔129/Sv-I1178NCADΔ small intestine revealed a variety of histologic abnormalities. The severity varied between the five ES cell lines but was identical for all mice derived from a given line. In the duodenum and proximal jejunum, cross-sections of some villi revealed bands of distended cells that lacked a distinctive brush border (Fig. 5 *B*). Some villi contained bands of enterocytes with normal morphology and adjacent bands of cells with large cytoplasmic vacuoles or enterocytes with a condensed cytoplasm and a pyknotic nucleus (Fig. 5 *C*). These latter features are consistent with entry into a death program. In the distal jejunum, villi often contained clusters of enterocytes that had lost their normal cell-cell contacts and appeared to be extruding into the lumen (Fig. 5 *D*). Villi in the proximal ileum contained groups of enterocytes that had lost their attachment to each other and to the underlying lamina propria (Fig. 5 *E*). Staining adjacent sections with UEA-1 allowed us to correlate all of these changes with a 129/Sv-I1178NCADΔ genotype.

Some jejunal villi contained bands of UEA-1–positive cells that had separated from the basement membrane, creating a highly vacuolated space between enterocytes and the villus core (Fig. 5 *F*). This separation was initially expressed as an increase in clear subnuclear vesicles in the lower third of the villus, followed by a more pronounced separation at the midpoint of the villus. The lamina propria side of the basement membrane was lined with mesenchymal cells (Fig. 5 *F*). While cell–matrix interactions were perturbed, cell–cell contacts appeared to be intact. One possible explanation for this phenotype was that the epithelial sheet had separated from the mesenchyme due to basement membrane dissolution. A study with cultured cells had shown previously that suppression of cadherin function results in secretion of a matrix-degrading, urokinase-type, plasminogen activator (Frixen and Nagamine, 1993). Therefore, sections containing polyclonal villi with these abnormalities were incubated with antisera specific for laminin, collagen type IV, or heparin sulfate proteoglycan. There were no detectable differences in the distribution or levels of these extracellular matrix components under UEA-1–positive 129/Sv-I1178NCADΔ-enterocytes and UEA-1–negative B6 enterocytes, indicating that the basement membrane was intact (data not shown).

Analysis of multiple UEA-1–positive ileal villi revealed that a range of phenotypes was often evident along the basilar-to-apical axis of a single villus (Fig. 5 *G*). Cells at the base of a villus were "piled-up" on each other. As cells migrated up the villus, vacuolated regions appeared between adjacent enterocytes and between enterocytes and the basement membrane (Fig. 5 *G*). Groups of enterocytes separated from the underlying lamina propria before they had reached the normal site of exfoliation at the apical extrusion zone (Fig. 5 *G*). These cells lost their differentiated phenotype as they approached the villus tip: i.e., they became spindle-shaped, brush border staining was weak to absent, and Golgi staining was disorganized. Some polyclonal ileal villi contained bands of UEA-1–positive cells that bore no resemblance to any of the known intestinal epithelial lineages. These cells were highly vacuolated and contained few discernable nuclei (Fig. 5, *H* and *I*).

---

border. (*C*) An ileal villus sectioned perpendicular to its crypt-villus axis. The arrows point to poorly adherent, rounded enterocytes with pynotic nuclei and condensed cytosplasm; (*D*) The bar identifies a group of enterocytes, located near the tip of a jejunal villus, that have lost their cell-cell contacts. (*E*) Arrows highlight the perturbations in enterocytic morphology and adhesion present in the upper half of an ileal villus. (*F-I*) Sections of B6↔129/Sv-I1178NCADΔ intestine recovered from a 6-wk-old animal, incubated with peroxidase-conjugated UEA-1 (visualized with DAB). (*F*) A sheet of UEA-1–positive 129/Sv-I1178NCADΔ enterocytes is separating from the underlying lamina propria. Cells located in the lower quarter of the villus contain subnuclear vacuoles (*closed arrows*). As these enterocytes migrate up the villus, they appear to become detached from the basement membrane (*closed arrowheads*). Mesenchymal cells have lined up against this membrane (*open arrows*). (*G*) A single proximal ileal villus displays a range of abnormalities. Open arrows point to aggregates of UEA-1–positive enterocytes that have piled up on one another at the base of the villus. The closed arrows point to vacuoles which have formed between, and within, enterocytes located in the mid and upper portions of the villus. Distinct staining of the supranuclear Golgi apparatus by UEA-1 is observed in enterocytes positioned within the lower half of the villus (*closed arrowheads*) but is lost as cells continue their upward migration. (*H*) Ileal villi sectioned perpendicular to the crypt-villus axis. The arrows point to a polyclonal villus which contains a band of UEA-1–negative, B6-derived enterocytes (*closed arrow*) and a band of vacuolated, UEA-1–positive, 129/Sv-I178NCADΔ cells (*open arrow*). (*I*) High power view of the polyclonal villus shown in *H* reveals that the UEA-1–positive, 129/Sv-I1178NCADΔ cells are filled with vacuoles, lack an organized Golgi apparatus, and bear no resemblance to normal enterocytes. The vacuoles fail to stain with PAS or Alcian Blue (data not shown). Bar in panel *A*, 25 μm.

Careful analysis of the duodenal-ileal axis of B6↔129/Sv-I1178NCADΔ mice failed to reveal any bands of B6 enterocytes with any of the histological abnormalities described above.

Loss of Cadherin-mediated Cell Adhesion Disturbs the Intestinal Epithelial Barrier. The integrity of the intestinal epithelial barrier is thought to be regulated by the highly organized apical junctional complex and its associated terminal web of microfilaments (cf Weiser et al., 1986; Madara, 1990). Electron microscopic studies of normal intestinal epithelial cells undergoing cell division or extrusion indicate that their apical junctional complexes are rapidly remodeled (Madara, 1990; Jinguji and Ishikawa, 1992). Experiments in cultured cells suggest that E-cadherin is essential for this type of remodeling (Gumbiner et al., 1988; Watabe et al., 1994). Therefore, we anticipated that disrupting cadherin function in enterocytes would greatly compromise barrier functions. Analysis of 6–8-wk-old B6↔129/Sv-I1178NCADΔ mice (n = 3–5 animals/cell line; 5 cell lines surveyed) revealed evidence of such compromise. First, as noted above, cell–cell contacts were disturbed. Second, PAS and Alcian blue staining disclosed that the surface mucus layer overlying 129/Sv-I1178NCADΔ but not B6 epithelium was disrupted (data not shown). This mucus layer protects the epithelium from mechanical, chemical, and microbiologic damage (Weiser et al., 1986). Third, clusters of Gram-negative bacteria were found infiltrating between poorly adherent villus-associated enterocytes (Fig. 6 *B*). Surveys of serial sections demonstrated that the bacteria were restricted to UEA-1–positive, 129/Sv-I1178NCADΔ cells. Flushing the intestine before fixation did not remove the bacteria. They were not detected in nonchimeric littermates housed in the same cage or in normal B6↔129/Sv mice, even when their luminal contents were not flushed before fixation (Fig. 6 *A*). These observations suggest that loss of cadherin function in 129/Sv-I1178NCADΔ enterocytes creates a favorable niche for bacteria. This niche could be created by loss of the surface mucus layer (Walker et al., 1985), changes in the carbohydrate composition of cell surface glycoconjugates which act as receptors for bacterial adhesins (Falk et al., 1995*b*), or disruptions of homotypic E-cadherin interactions which allow the protein's extracellular domain to then serve as a receptor for bacterial adhesins (Sansonetti et al., 1994). Fourth, there were localized increases in the number of lymphocytes present in the lamina propria of polyclonal villi or in villi composed entirely of 129/Sv-I1178NCADΔ enterocytes. Massive lymphoid aggregates were found protruding into the bowel wall, some without an overlying follicle-associated epithelium characteristic of Peyer's patches. These aggregates were associated with 129Sv-I1178NCADΔ-epithelium. They were not present in nonchimeric littermates housed in the same microisolator cages or in normal, age-matched B6↔129/Sv chimeras maintained in the same barrier facility. Their presence could reflect entry of bacteria and/or other luminal antigens through direct breaches in the epithelial barrier. They can not be ascribed to an immunologic response to the *Xenopus* NCADΔ itself since I-FABP$^{-1178\ to\ +28}$ is activated on embryonic day 15, well before development of the immune repertoire in mice (e.g., for reviews see Goodnow, 1992; Lo, 1992).

Mechanisms

The Levels and Distribution of Endogenous Cadherins. To begin to explore the mechanisms responsible for producing these changes in differentiation and adhesion, sections were prepared from the small intestine of 6–8-wk-old B6↔129/Sv-I1178NCADΔ mice that had been generated with two independent ES cell lines (n = 3 mice/cell line; 30–50% 129/Sv). Fig. 2 *D* shows a polyclonal ileal villus incubated with the E-cadherin mAb and UEA-1. E-cadherin is concen-

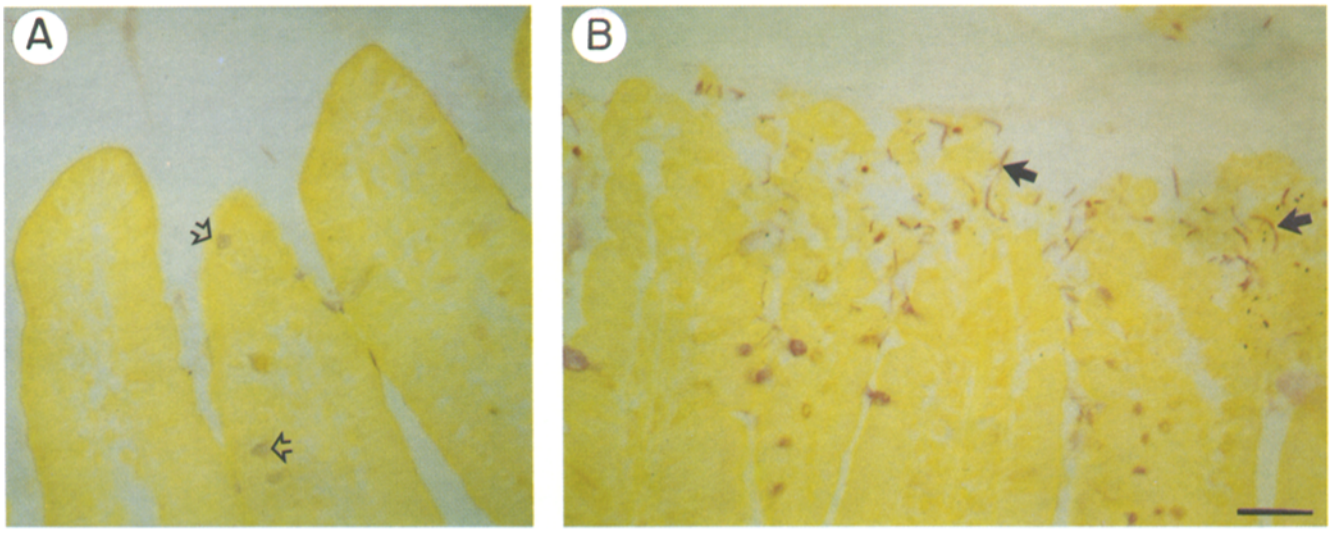

Figure 6. Adult B6↔129/Sv-I1178NCADΔ mice exhibit alterations in their intestinal epithelial barrier functions. (*A*) Gram stain of a section of ileum from a normal 8-wk-old B6↔129/Sv mouse. The intestine was not perfused with PBS before fixation. No bacteria are evident. Note the absence of extrusion of cells from the villus tip. Goblet cells contain light purple colored mucus droplets (*open arrows*). (*B*) Gram stain of a section of ileum from an 8-wk-old B6↔129/Sv-I1178NCADΔ mouse. Numerous Gram-negative bacteria (*purple*; *arrows*) surround villus tips containing disrupted, nonadherent enterocytes. These bacteria were seen whether or not the intestine was perfused with PBS before fixation. Bar, 25 μm.

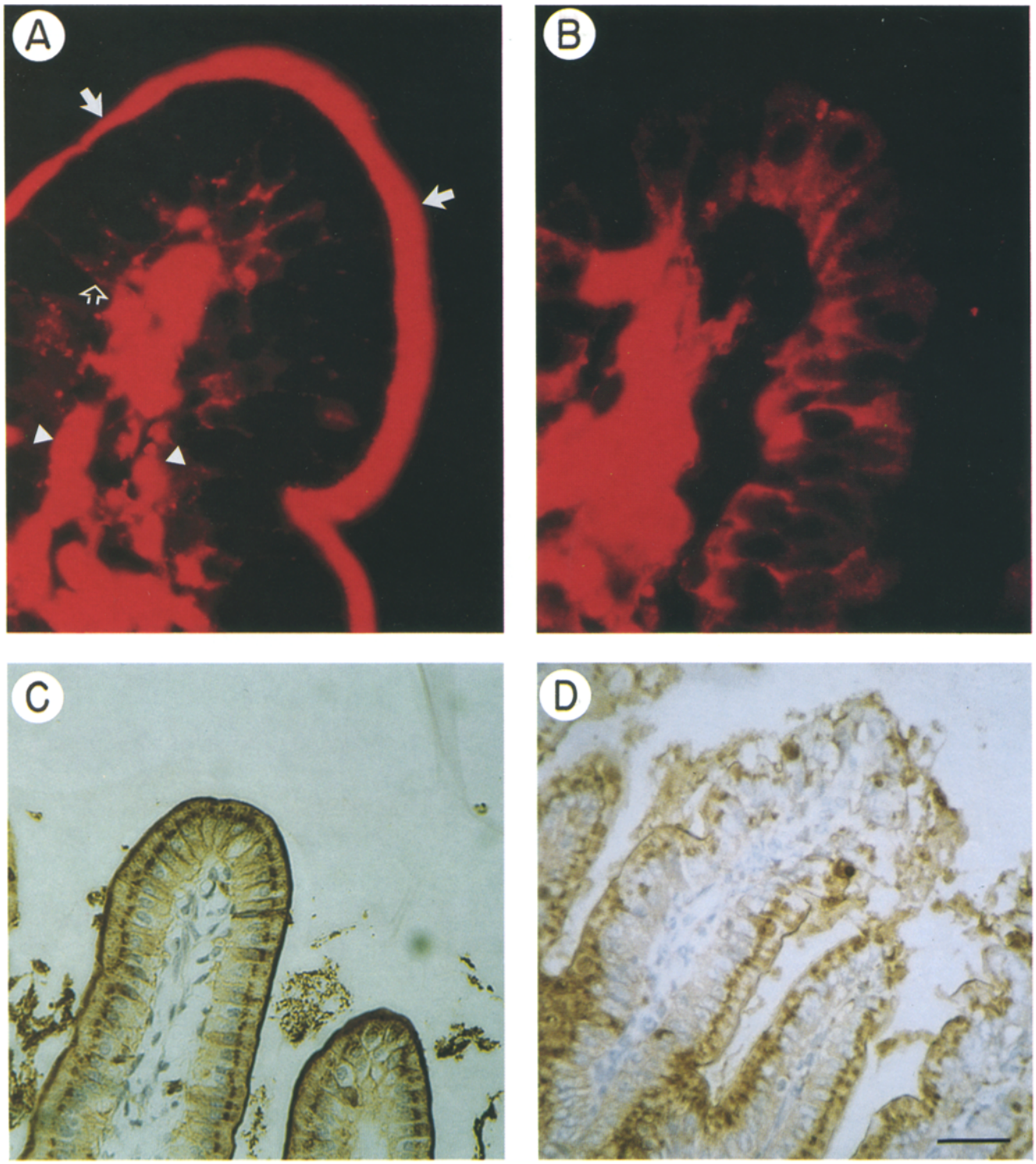

Figure 7. NCADΔ expression is associated with disruption of the actin cytoskeleton and loss of polarity in villus-associated enterocytes. (*A*) Section prepared from the proximal ileum from a B6↔129/Sv mouse and stained with a mouse β-actin mAb (visualized with Cy3-labeled sheep anti-mouse Ig). A prominent band of immunoreactive protein is associated with the terminal web and brush border of enterocytes located at the villus tip (*closed arrows*). Weak staining is detectable along the basolateral surfaces of these cells (e.g., *open arrow*). Lymphocytes located in the lamina propria (*closed arrowheads*) react with the sheep anti-mouse Ig. (*B*) Section of a proximal ileal villus from a B6↔129/Sv-I1178NCADΔ mouse. Apical brush border and terminal web staining is absent. There is pronounced increase in immunoreactive β-actin in the cytoplasm of these 129/Sv-I1178NCADΔ enterocytes. (*C*) Section containing proximal ileal villi from the normal B6↔129/Sv mouse shown in *A*. The section was incubated with peroxidase-conjugated *Glycine max* agglutinin (GMA; visualized with DAB; counterstain = hematoxylin). There is prominent staining of glycoconjugates located in the apical brush border and supranuclear Golgi apparatus. (*D*) Section of proximal ileum from the mouse in *B*. The section is stained with GMA as in *C*. As 129/Sv-I1178NCADΔ enterocytes migrate up the villus, they lose their distinctive Golgi and brush border staining and acquire cytoplasmic vacuoles that do not react with the lectin. Bar, 25 μm.

trated at points of contact between normal B6 enterocytes. E-cadherin levels increase as these cells migrate toward the villus tip. The steady state level of E-cadherin is reduced dramatically in the adjacent band of 129/Sv-I1178NCADΔ enterocytes. Abnormal, subnuclear clumps of E-cadherin immunoreactivity were observed in UEA-1–positive enterocytes, especially if the cells had separated from the underlying mesenchyme (Fig. 2 *E*).

Sections were also incubated with the pan-cadherin antisera that reacts with the cytoplasmic domains of NCADΔ and endogenous wild-type cadherins. Despite the decrease in E-cadherin levels (Fig. 2 *D*), total cellular cadherin concentrations (NCADΔ plus endogenous cadherins) were increased in villus-associated 129/Sv-I1178NCADΔ compared to B6 enterocytes (Fig. 2, *C* and *F*). This finding established that the I1178NCADΔ transgene was actively expressed in 129/Sv enterocytes. In addition, the pan-cadherin antibody revealed large clumps of immunoreactive protein in 129/Sv-I1178NCADΔ enterocytes at sites of cell–cell contact and throughout their cytoplasm (compare panels *F* and *C* in Fig. 2). Adjacent bands of B6 enterocytes, as well as epithelial cells in B6 and 129/Sv-I1178NCADΔ crypts, had no detectable abnormalities in the level or intracellular distribution of cadherins (data not shown).

Actin Distribution and Cell Polarity. α-Catenin, β-catenin, and γ-catenin bind to the cytosolic domain of E-cadherin and link it to the cytoskeleton (Ozawa et al., 1989; Nagafuchi and Takeichi, 1988). Studies with cultured cells indicate that the interactions between cadherins, catenins, and the actin-based cytoskeleton are essential for cell adhesion and maintenance of cell polarity (Nagafuchi and Takeichi, 1988; Ozawa et al., 1990; Watabe et al., 1994). Therefore, sections of normal B6↔129/Sv and B6↔129/Sv-I1178NCADΔ jejunum and ileum were incubated with a mouse β-actin mAb. The results indicate that the actin cytoskeleton becomes disorganized as contact is diminished between 129/Sv-I1178NCADΔ enterocytes during their migration up the villus: β-actin levels are reduced and the protein's distinctive localization at the terminal web is replaced by a diffuse cytoplasmic distribution (compare panels *A* and *B* in Fig. 7).

Actin may be particularly important for maintaining polarity in enterocytes, since it is the predominant component of microvilli and the terminal web (Drenckhahn and Dermietzel, 1988). Lectins are remarkably sensitive tools for defining variations in the differentiation program of each of the intestine's four principal cell lineages and for identifying changes in protein compartmentalization (Falk et al., 1994, 1995*a*). The *N*-acetyl-D-galactosaminyl-specific soybean lectin, *Glycine Max* agglutinin (GMA) recognizes glycoconjugates that accumulate in the apical brush border and Golgi apparatus of enterocytes (Falk et al., 1994). 129/Sv-I1178-NCADΔ enterocytes have markedly decreased or absent brush border staining with GMA. Moreover, Golgi staining is punctate and disorganized compared to B6 enterocytes (Fig. 7, *C* and *D*). Similar results were obtained with four other lectins that have distinct carbohydrate specificities—*Helix promentia* agglutinin, *Artrocarpus integrifolia* agglutinin, *Dolicos biflorus* agglutinin, and *Moluccella laevis* lectin. These findings are consistent with a defect in the polarized sorting of apical membrane proteins in NCADΔ-producing enterocytes.

NCADΔ-mediated perturbations of the cytoskeleton and polarized distribution of cellular proteins may have contributed to the high incidence of neonatal lethality observed in our pilot experiments. Limited analyses of moribund postnatal day 1 animals revealed numerous villi with bands of grossly disturbed cells having characteristics similar to those observed in the proximal ileum of adult low percent B6↔129/Sv-I1178NCADΔ chimeras (Fig. 5, *G–I*). The absence of an organized enterocytic brush-border membrane is a feature of microvillus inclusion disease, an autosomal recessive disorder associated with high infant mortality (Cutz et al., 1989).

Together, these findings indicate that endogenous cadherins are needed to maintain an enterocyte's polarity during its 48 h residence on the villus. The findings also lend support to the notion that differentiation of this lineage is not an autonomous process (Duluc et al., 1994) but rather an active process supported by a molecular cross talk which includes cadherin-dependent cell–cell and/or cell–matrix interactions.

Cell Proliferation in Crypts. Analysis of hematoxylin- and eosin-stained sections prepared from the most perturbed regions of B6↔129/Sv-I1178NCADΔ intestine indicated that crypts were deeper and had increased numbers of M-phase cells (mean = 4 mitotic figures/longitudinal crypt section in B6↔129/Sv-I1178NCADΔ ileum compared to 1 mitotic figure/ileal crypt in comparably aged B6↔129/Sv mice; n = 30 crypt sections counted per mouse; 2 mice/genotype) (Fig. 8, *A* and *B*). Increased proliferation in ES-derived crypts is noteworthy since I-FABP$^{-1178\text{ to }+28}$ is not active in their epithelial cell populations. It suggests that there is a signaling pathway which operates along the crypt-villus axis to sense any changes in the census of villus-associated enterocytes,

Figure 8. Disrupting cadherin function results in increased proliferation in crypts, an increased rate of cell migration, and precocious induction of programmed cell death. (*A*) Hematoxylin- and eosin-stained section of ileal crypts from a 6-wk-old B6↔129/Sv chimeric mouse. (*B*) Section from a comparably aged B6↔129/Sv-I1178NCADΔ chimeric-transgenic animal showing hyperproliferative ileal crypts. M-phase cells are more prevalent (*closed arrows*) and the crypts are deeper. The sections shown in *A* and *B* were prepared from the same position along the duodenal-ileal axis and photographed at the same magnification. (*C*) Section of a polyclonal jejunal villus from a 6-wk-old B6↔129/Sv-I1178NCADΔ mouse injected with BrdU 60 h before sacrifice. The section was incubated with goat anti-BrdU (visualized with Cy3-conjugated donkey anti-goat Ig). Arrows point to the lagging edges of the migrating bands of BrdU-positive (*red*) cells. (*D*) Double exposure of the same section as shown in *C* after staining with biotin-conjugated UEA-1 (visualized with FITC-conjugated extravidin). A comparison of *C* and *D* demonstrates that BrdU-positive 129/Sv-I1178NCADΔ enterocytes (*yellow-green plus red*) are located higher up on the villus than BrdU-positive B6 enterocytes (*red only*). (*E*) Section of ileum from a B6↔129/Sv-I1178NCADΔ mouse stained with anti-BrdU sera (visualized as in *C*). The closed arrows point to BrdU-positive cells with nuclear DNA fragmentation suggesting programmed cell death. (Double staining with UEA-1 established that these cells had a 129/Sv-I1178NCADΔ genotype, data not shown). (*F*) A TUNEL assay performed on a section of B6↔129/Sv-I1178NCADΔ ileum (counterstained with crystal violet). Reconstruction of serial sections revealed that the band of TUNEL-positive (apoptotic) cells (*dark brown, closed arrows*) had a 129/Sv-I1178NCADΔ genotype. Note that no TUNEL-positive cells are detectable in an adjacent band of B6 enterocytes located on the same polyclonal villus. Bar, 25 μm.

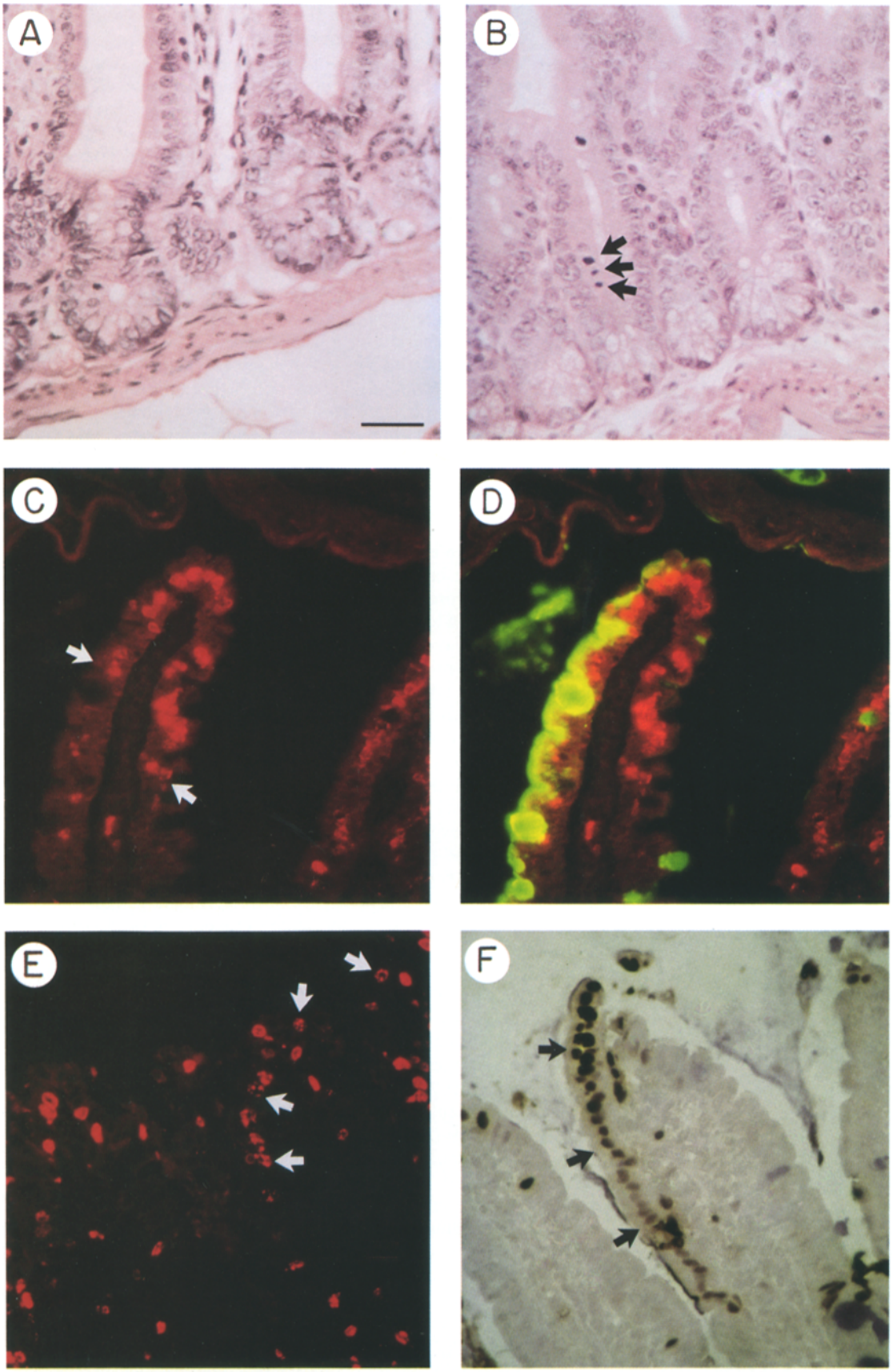
A
B
C
D
E
F

their state of differentiation, their rate of exfoliation, and/or their death programs, and to initiate compensatory proliferative responses. The nature of this pathway remains to be defined.

Migration Rates and Apoptosis. As noted above, analysis of intestinal wholemounts and tissue sections revealed that NCADΔ production does not affect villus height. An increase in crypt cell production without a concommitent change in villus height could reflect a number of mechanisms: (*a*) NCADΔ-producing enterocytes could migrate more rapidly along the crypt-villus axis and be extruded at an accelerated rate from the apex of the villus and/or (*b*) NCADΔ-positive enterocytes could be lost during their migration along the villus, either through extrusion at ectopic sites and/or by precocious entry into a death program.

To determine if NCADΔ disturbed migration rates, we first analyzed migration rates in 6-wk-old normal B6 mice and in B6↔129/Sv chimeras. Animals were given a single intraperitoneal injection of the thymidine analog 5′-bromo-2′-deoxyuridine (BrdU) to label crypt epithelial cells during S-phase. Mice were sacrificed 1.5, 6, 12, 24, 48, 60, 72, or 96 h later and sections of crypt-villus units in duodenal, jejunal, and ileal segments were incubated with an anti-BrdU sera to determine the distance that BrdU-labeled cells had migrated. In all regions of the duodenal-ileal axis, enterocytes located at the leading edge of the band of BrdU-positive cells reach the crypt-villus junction within 12 h while the lagging edge of the band passes through this junction within 48 h. In the ileum, the leading edge of BrdU-positive enterocytes reaches the villus tip by 60 h. At this time point, the band of BrdU-positive cells covers the upper two thirds of the villus. By 72 h, only the upper quarter of ileal villi contain labeled cells, indicating that a large number of enterocytes have been extruded from the villus tip. In the duodenum and jejunum where villi are longer, BrdU-labeled cells take 60 h to arrive at midportion of the villus, 72 h to reach the villus tip, and are rarely seen at 96 h (data not shown). These migration rates are not affected by genetic background: the number of labeled cells/crypt-villus unit/time point, and the distance they migrate/unit of time are the same for UEA-1-positive 129/Sv-enterocytes and for UEA-1-negative B6 enterocytes located on the same polyclonal villus (data not shown).

When B6↔129/Sv-I1178NCADΔ mice were sacrificed 60 h after treatment with BrdU, it was apparent that the band of BrdU-labeled enterocytes in a 129/Sv-I1178NCADΔ-stripe was significantly shorter than the band of BrdU-labeled cells in an adjacent B6 stripe. For example, BrdU-labeled UEA-1-positive cells were located in the upper quarter of an ileal villus, a position normally only reached after 72 h in normal 129/Sv ileal villi. In contrast, two thirds of the adjacent B6-derived stripe contained labeled cells ($n = 4$ comparably aged mice derived from two independent 129/Sv-I1178NCADΔ cell lines; at least 10 polyclonal villi surveyed/animal; e.g., see Fig. 8, *C* and *D*). These results indicate that 129/Sv-I1178NCADΔ enterocytes migrate at an accelerated rate.

A large number of BrdU-positive 129/Sv-I1178NCADΔ enterocytes in distal jejunal and ileal villi had fragmented appearing nuclei, suggesting entry into a cell death program (Fig. 8 *E*). TdT-mediated dUTP-nick end labeling (TUNEL) assays were performed to evaluate this finding further (Gavrieli et al., 1992; Hall et al., 1994). In normal 6–8-wk-old B6↔129/Sv mice, this assay only labels a few cells located at the extreme tips of villi plus a few scattered cells in the crypts (data not shown). In age-matched B6↔129/Sv-I1178NCADΔ mice, bands of UEA-1–positive enterocytes were often labeled in the TUNEL assay (Fig. 8 *F*). In some cases, these bands of TUNEL-positive cells extended along the entire length of the villus. This pattern of labeling was not evident in adjacent B6 enterocytes (Fig. 8 *F*). It is important to note that these increases in apoptosis were only observed in those areas of the duodenal-ileal axis where cell–cell adhesion was most severely disrupted (i.e., proximal ileum; $n = 6$ mice representing 3 independent ES cell lines). When cell–matrix interactions were disrupted without associated loss of cell–cell contacts (e.g., the jejunal villus shown in Fig. 5 *F*), bands of TUNEL-positive cells were never found. Together, these data indicate that loss of cadherin-mediated cell–cell contacts produces precocious induction of programmed cell death and suggests that cadherins can function as survival factors for enterocytes in vivo.

Discussion

We have expressed a dominant-negative N-cadherin mutant protein in postmitotic, villus-associated enterocytes. Our results provide an in vivo demonstration that cadherins can function to actively maintain the state of differentiation of an epithelial cell lineage, to control its adhesive properties and rate of migration, and to regulate its death program.

The Effect of NCADΔ on Enterocyte Adhesion and Migration. Cell adhesion has been disrupted by expressing a N-cadherin mutant lacking the extracellular domain in *Xenopus* embryos (Kinter, 1992; Dufour et al., 1994; Holt et al., 1994), in a mouse keratinocyte cell line (Fujimori and Takeichi, 1993), and now in villus-associated enterocytes. When expressed at high levels, *Xenopus* NCADΔ competes with and prevents α-catenin binding to E-cadherin in *Xenopus* embryos (Kinter, 1992). In contrast, expression of a comparable chicken N-cadherin dominant-negative mutant in the mouse keratinocyte cell line does not appear to alter interactions between endogenous cadherins and catenins. Rather, immunocytochemical studies demonstrated that production of this NCADΔ mutant results in a pronounced reduction in the levels of endogenous mouse E-cadherin at sites of cell–cell contact (Fujimori and Takeichi, 1993). We noted a similar reduction in endogenous E-cadherin levels when NCADΔ expression was directed to villus-associated mouse enterocytes in vivo (Fig. 2, *D* and *E*). Fujimore and Takeichi (1993) hypothesized that (*a*) NCADΔ may replace endogenous cadherin-catenin complexes at adherens junctions and (*b*) the mutant protein may interfere with formation of large supramolecular E-cadherin arrays (cores) which develop after intact endogenous cadherins initially accumulate at sites of cell–cell contact through their intercellular homophilic interactions. They proposed that this interference could actively remove preexisting endogenous cadherins from these sites of cell–cell contact if the mutant cadherin has a higher affinity for cytoskeletal "receptors." The presence of complexes composed of a mutant cadherin that lacks an extracellular domain prevents cell adhesion. Our results support these notions. Studies with an E-cadherin mAb disclosed that cellular E-cadherin levels are reduced at the

basolateral surfaces of villus-associated 129/Sv-NCADΔ enterocytes. Moreover, when a pan-cadherin antibody was used to monitor the distribution of NCADΔ (plus endogenous cadherins), we noted (*a*) a pronounced increase in total cellular cadherin levels; (*b*) more immunoreactive protein at sites of cell–cell contact; and (*c*) an abnormal cytoplasmic distribution (Fig. 2 *F*).

Assembly of endogenous cadherin-catenin complexes appears to be a dynamic process. Large pools of cadherin-bound and cadherin- independent catenins are present in cultured cells (Hinck et al., 1994; Näthke et al., 1994). Several observations support the hypothesis that endogenous cadherins and cadherin-catenin complexes must turn over before a critical mass of NCADΔ can accumulate at specific sites within enterocytes to disrupt adhesion. I-FABP$^{-1178\ to\ +28}$/reporter transgenes are turned on at the crypt-villus junction and expression is sustained until cells are exfoliated at the villus tip yet there is gradient of phenotypic abnormalities observed in 129/Sv-I1178NCADΔ enterocytes along the villus. Severe disruption of adhesion is not apparent until cells reach the upper half to third of the villus and these adhesive defects are associated with abnormal patterns of pan-cadherin staining. Pulse-chase experiments with BrdU show that it takes cells ~4–6 h to travel from the crypt-villus junction to the point on the villus where disturbances in cadherin-staining patterns and adhesion are first detectable. This interval is approximately equal to the turnover time for E-cadherin-catenin complexes measured in cultured epithelial cells (Hinck et al., 1994).

Schmidt et al. (1993) proposed that since integrin-mediated focal contacts and cadherin-mediated adherens junctions share the same G-actin pool, focal plaques between cells and the extracellular matrix form at the expense of adherens junctions between cells, and vice versa. This model predicts stronger contacts between cells and the extracellular matrix when cadherin-mediated cell–cell contacts are disrupted. In contrast, our data reveal that NCADΔ-producing enterocytes are less tightly adherent to the basement membrane. This suggests that integrins cannot compensate for the loss of cadherin function. However, disrupting cadherin-dependent organization of the cytoskeleton may perturb integrin-mediated interactions between the extracellular matrix and the cytoskeleton at basolateral focal contacts. Cadherins are known to affect integrin function. Experiments with cultured human keratinocytes have shown that inhibition of E-cadherin function with blocking antibodies slows the redistribution of β_1 integrin during the initial phases of Ca^{2+}-induced cell adhesion and prevents its down-regulation during cell stratification (Wheelock and Jensen, 1992; Hodivala and Watt, 1994). Transfection of α-catenin deficient PC9 lung carcinoma cells with an α-catenin DNA permits activation of E-cadherin–dependent functions and results in the formation of cell–cell contacts plus β1, α2, α3, and α6 integrin redistribution to the basolateral surface (Watabe et al., 1994). The "loosening" of cell-extracellular matrix interactions may explain the accelerated migration of NCADΔ-enterocytes along the crypt-villus axis as well as the loss of sheets of cells (e.g., Fig. 5 *F*). This notion is supported by the finding that a dominant-negative β1B integrin reduces spreading and motility in CHO cells (Balzac et al., 1994). Examination of the effect of NCADΔ on the levels and distribution of integrins in B6↔129/Sv-I1178NCADΔ mice should provide information about the validity of this hypothesis.

Cadherins May Function as Cell Survival Factors That Prevent Precocious Programmed Cell Death: Implications for the Pathogenesis of Intestinal Neoplasia. Death programs may be activated or suppressed by signals from the environment and prevention of programmed cell death may require continuous inhibition by locally acting "survival factors" (Raff, 1992). Loss of integrin-mediated cell–cell or cell–matrix contacts can lead to apoptosis in cultured cells (Meredith et al., 1993; Bates et al., 1994; Frisch and Francis, 1994; Montgomery et al., 1994; Re et al., 1994). This phenomenon has been termed "anoikis" and may be a normal mechanism which prevents cellular reattachment at inappropriate sites, thereby maintaining proper tissue organization and cellular census (Raff, 1992; Frisch and Francis, 1994; Ruoslahti and Reed, 1994).

Morphological as well as DNA fragmentation data indicate that programmed cell death is normally restricted to the apical extrusion zone located at the villus tip (Gavrelli et al., 1992; Hall et al., 1994). Analysis of B6↔129/Sv-I1178NCADΔ mice revealed that loss of cadherin-mediated cell–cell and/or cell–matrix interactions can trigger induction of programmed cell death along the entire villus. This suggests that entry into an apoptotic pathway is actively suppressed in cells distributed along the length of the villus and that cadherins represent one class of survival factors essential for active suppression of this death program. The nuclear organization of enterocytes distributed along the villus of normal B6↔129/Sv mice suggests that preparation for death is a normal part of the lineage's terminal differentiation program: i.e., chromatin condensation and nuclear marginalization, early markers of apoptosis (Wyllie et al., 1980), accompanies migration-associated differentiation (Fig. 5 *A*).

Functional E-cadherin complexes contain either α- and β-catenin, or α-catenin and plakoglobin (Hinck et al., 1994). If these complexes are negative regulators of cell death in villus-associated enterocytes, then it is possible that the tumor suppressor APC could be a positive regulator of death. APC and E-cadherin compete for binding to the same internal, *armadillo*-like repeats of β-catenin (Hülsken et al., 1994; Rubinfeld et al., 1993; Su et al., 1993). Therefore, a dynamic equilibrium may exist between pools of free β-catenin, β-catenin:E-cadherin complexes, and β-catenin:APC complexes (Hinck et al., 1994; Hülsken et al., 1994). We hypothesize that a shift in the equilibrium towards β-catenin:E-cadherin complexes may promote cell survival while a shift in the equilibrium towards APC:β-catenin could promote cell death. One way the β-catenin:APC complex could initiate apoptosis is through an α-catenin–mediated effect on the cytoskeleton since it has been shown that disruption of microfilaments results in apoptosis in vitro (Kolber et al., 1990).

The distribution of APC in colonic crypts and the effects of its inactivation are consistent with a role in preparing for cell death during terminal differentiation. APC is restricted to the basolateral surface of (human) colonocytes. Levels increase as these cells complete their migration-associated differentiation (Smith et al., 1993). Inactivation of APC appears to be an early event in the multistep journey to human colorectal neoplasia (Fearon and Vogelstein, 1990) and produces multiple small intestinal and colonic adenomas in

the *Min* mouse (Moser et al., 1990, 1992; Su et al., 1992). Since death is essential for maintaining appropriate cellular census, loss of such control would, at the very least, lead to hyperplasia.

Loss of E-cadherin function alone appears insufficient to produce intestinal neoplasms. Extensive analysis of 6–8-wk-old B6↔129/Sv-I1178NCADΔ mice (n = 15 animals derived from 5 stably transfected ES cell lines) failed to reveal any evidence of adenomas or carcinoma. Loss of cadherin-mediated cell adhesion is a late, rather than early, event in oncogenesis and correlates with tumor cell dedifferentiation in vitro and in vivo (Vleminckx et al., 1991; Frixen et al., 1991; for a review see Takeichi, 1993). Loss of potential death inducers such as APC and/or p53 may be needed before inactivation of E-cadherin can produce intestinal neoplasia. This could be tested by generating chimeric-transgenic mice with ES cells that contain both I-FABP$^{-1178\text{ to }+28}$/NCADΔ and *Apc*^{Min} and noting if intestinal adenomas form earlier in postnatal life, if their numbers increase, or if they show a more malignant phenotype than in mice which only contain *Apc*^{Min}. Alternatively, the lack of intestinal neoplasms in B6↔129/Sv-I1178NCADΔ mice may be due to the inability of "initiated" NCADΔ-producing enterocytes to achieve functional anchorage during their accelerated migration along the villus. Previous studies have shown that the expression of several oncogenes in villus-associated enterocytes can lead to their reentry into the cell cycle and dedifferentiation but not to neoplasia (Kim et al., 1993, 1994). The site of initiation of tumorigenesis in the gut may have to be the functionally anchored stem cell or one of its immediate descendants (Kim et al., 1993). Anchorage may be possible to genetically engineer outside of the stem cell zone if overexpression of E-cadherin is shown to retard migration rate along the crypt-villus axis.

Prospectus. Further immunocytochemical studies of the polyclonal villi in these chimeric-transgenic mice should help clarify the effect of loss of cadherin function on proteins such as APC, catenins, various adhesion molecules (e.g., integrins, ZO-1), and tyrosine kinases located at adherens junctions (for a review see Ranscht, 1994). The results of such analyses should provide a conceptual basis for generating additional types of chimeric-transgenic mice to test the functions of proteins postulated to act upstream, downstream, or in parallel with cadherins to regulate the continuum of cell birth to cell death which exists along the crypt-villus axis (e.g., β-catenin; cf McCrea et al., 1993; Peifer et al., 1993). Finally, the experiments described in this report have examined the role of cadherins in a differentiated cell lineage. It will be important to use other well defined promoters (Cohn et al., 1992; Simon et al., 1993; Crossman et al., 1994) to direct expression of NCADΔ to crypts as well as to villus-associated epithelial cells and assess the effects on establishment and maintenance of crypt-villus units.

The authors are indebted to Dave O'Donnell for his expert technical assistance, members of our lab for their many stimulating discussions, and Rolf Kemler and Chris Kinter for generously supplying us with needed reagents.

This work was supported in part by grants from the National Institutes of Health (DK37960 and DK30292).

Received for publication 7 December 1994 and in revised form 1 February 1995.

References

Balzac, F., S. F. Retta, A. Albini, A. Mechiorri, V. E. Koteliansky, M. Geuna, L. Silengo, and G. Tarone. 1994. Expression of β1B integrin isoform in CHO cells results in a dominant negative effect on cell adhesion and motility. *J. Cell Biol.* 127:557–565.

Bates, R. C., A. Buret, D. F. van Helden, M. A. Horton, and G. F. Burns. 1994. Apoptosis induced by inhibition of intercellular contact. *J. Cell Biol.* 125:403–415.

Behrens, J., W. Birchmeier, S. L. Goodman, and B. A. Imhof. 1985. Dissociation of Madin-Darby canine kidney epithelial cells by the monoclonal antibody anti-arc-1: mechanistic aspects and identification of the antigen as a component related to uvomorulin. *J. Cell Biol.* 101:1307–1315.

Behrens, J., M. M. Mareel, F. M. Van Roy, and W. Birchmeier. 1989. Dissecting tumor cell invasion: epithelial cells acquire invasive properties after the loss of uvormorulin-mediated cell–cell adhesion. *J. Cell Biol.* 108:2435–2447.

Berndorff, D., R. Gessner, B. Kreft, N. Schnoy, A.-M. Lajous-Petter, N. Loch, W. Reutter, M. Hortsch, and R. Tauber. 1994. Liver-intestine cadherin: molecular cloning and characterization of a novel Ca^{2+}-dependent cell adhesion molecule expressed in liver and intestine. *J. Cell Biol.* 125:1353–1369.

Boller, K., D. Vestweber, and R. Kemler. 1985. Cell-adhesion molecule uvomorulin is localized in the intermediate junctions of adult intestinal epithelial cells. *J. Cell Biol.* 100:327–332.

Bradley, A. 1987. Production and analysis of chimaeric mice. *In* Teratocarcinomas and Embryonic Stem Cells: a Practical Approach. E. J. Robertson, editor. IRL Press, Oxford, England, pp. 113–151.

Bry, L., P. Falk, K. Huttner, A. Ouellete, T. Midtvedt, and J. I. Gordon. 1994. Paneth cell differentiation in the developing intestine of normal and transgenic mice. *Proc. Natl. Acad. Sci. USA.* 91:10335–10339.

Cheng, H. 1974. Origin, differentiation and renewal of the four main epithelial cell types in the mouse small intestine. IV. Paneth cells. *Am. J. Anat.* 141:521–536.

Cheng, H., and Leblond. 1974. Origin, differentiation and renewal of the four main epithelial cell types in the mouse small intestine. I. Columnar cells. *Am. J. Anat.* 141:461–480.

Cohn, S. M., and M. W. Lieberman. 1984. The use of antibodies to 5'-bromo-2'deoxyuridine for the isolation of DNA sequences containing excision-repair sites. *J. Biol. Chem.* 25:12456–12462.

Cohn, S. M., T. C. Simon, K. A. Roth, E. H. Birkenmeier, and J. I. Gordon. 1992. Use of transgenic mice to map *cis*-acting elements in the intestinal fatty acid binding protein gene (*Fabpi*) that control its cell lineage-specific and regional patterns of expression along the duodenal-colonic and crypt-villus axes of the gut epithelium. *J. Cell Biol.* 119:27–44.

Crossman, M. W., S. M. Hauft, and J. I. Gordon. 1994. The mouse ileal lipid binding protein gene: a model for studying axial patterning during gut morphogenesis. *J. Cell Biol.* 126:1547–1564.

Cutz, E., J. M. Rhoads, B. Drumm, P. M. Sherman, P. R. Durie, and G. G. Forstner. 1989. Microvillus inclusion disease: an inherited defect of brush-border assembly and differentiation. *N. Engl. J. Med.* 320:646–651.

Dantzig, A. H., J. Hoskins, L. B. Tabas, S. Bright, R. L. Shepard, I. L. Jenkins, D. C. Duckworth, J. R. Sportsman, D. Mackensen, P. J. Rosteck, et al. 1994. Association of intestinal peptide transport with a protein related to the cadherin superfamily. *Science (Wash. DC).* 264:430–433.

Doetschman, T. C., H. Eistetter, M. Katz, W. Schmidt, and R. Kemler. 1985. The in vitro development of blastocyst-derived embryonic stem cell lines: formation of visceral yolk sac, blood islands, and myocardium. *J. Embryol. Exp. Morph.* 87:27–45.

Drenckhahn, D., and R. Dermietzel. 1988. Organization of the actin filament cytoskeleton in the intestinal brush border: a quantitative and qualitative immunoelectron microscope study. *J. Cell Biol.* 107:1037–1048.

Dufour, S., J.-P. Saint-Jeannet, F. Broders, D. Wedlich, and J. P. Thiery. 1994. Differential perturbations in the morphogenesis of anterior structures induced by overexpression of truncated XB- and N-cadherins in *Xenopus* embryos. *J. Cell Biol.* 127:521–535.

Duluc, I., J.-N. Freund, C. Leberquier, and M. Kedinger. 1994. Fetal endoderm primarily holds the temporal and positional information required for mammalian intestinal development. *J. Cell Biol.* 126:211–221.

Falk, P., K. A. Roth, and J. I. Gordon. 1994. Lectins are sensitive tools for defining the differentiation programs of mouse gut epithelial cell lineages. *Am. J. Physiol. (Gastrointest. Liver Physiol.).* 266:G987–G1003.

Falk, P. G., R. G. Lorenz, N. Sharon, and J. I. Gordon. 1995*a*. The *Moluccella laevis* lectin-a marker for cellular differentiation programs in the gastric and intestinal epithelium of developing and adult, normal and transgenic mice. *Am. J. Physiol.* 268:G553–G567.

Falk, P. G., L. Bry, J. Hogersson, and J. I. Gordon. 1995*b*. Expression of a human α1,3/4 fucosyltransferase in the pit cell lineage of FVB/N mouse stomach results in production of Lewis^b containing glygoconjugates: a potential transgenic mouse model for studying *Helicobacter pylori* infection. *Proc. Natl. Acad. Sci. USA.* 92:1515–1519.

Fearon, E. R., and B. Vogelstein. 1990. A genetic model for colorectal tumorigenesis. *Cell.* 61:759–767.

Frisch, S. M., and H. Francis. 1994. Disruption of epithelial cell-matrix interactions induces apoptosis. *J. Cell Biol.* 124:619–626.

Frixen, U. H., and Y. Nagamine. 1993. Stimulation of urokinase-type plasminogen activator expression by blockage of E-cadherin-dependent cell-cell adhesion. *Cancer Res.* 53:3618–3623.

Frixen, U. H., J. Behrens, M. Sachs, G. Eberle, B. Voss, A. Warda, D. Löchner, and W. Brichmeier. 1991. E-cadherin-mediated cell–cell adhesion prevents invasiveness of human carcinoma cells. *J. Cell Biol.* 113:173–185.

Fujimori, T., and M. Takeichi. 1993. Disruption of epithelial cell-cell adhesion by exogenous expression of a mutated nonfunctional N-cadherin. *Mol. Biol. Cell.* 4:37–47.

Gavrieli, Y., Y. Sherman, and S. A. Ben-Sasson. 1992. Identification of programmed cell death in situ via specific labeling of nuclear DNA fragmentation. *J. Cell Biol.* 119:493–501.

Geiger, B., T. Volberg, D. Ginsberg, S. Bitzur, I. Sabanay, and R. O. Hynes. 1990. Broad spectrum pan-cadherin antibodies, reactive with the C-terminal 24 amino acid residues of N-cadherin. *J. Cell Sci.* 97:607–614.

Goodnow, C. C. 1992. Transgenic mice and analysis of B cell tolerance. *Annu. Rev. Immunol.* 10:489–518.

Griffiths, D. F. R., S. J. Davies, D. Williams, G. T. Williams, and E. D. Williams. 1988. Demonstration of somatic mutation and colonic crypt clonality by x-linked enzyme histochemistry. *Nature (Lond.).* 333:461–463.

Gumbiner, B., and K. Simons. 1986. A functional assay for proteins involved in establishing an epithelial occluding barrier: identification of a uvomorulin-like polypeptide. *J. Cell Biol.* 102:457–468.

Gumbiner, B., B. Stevenson, and A. Grimaldi. 1988. The role of the cell adhesion molecule uvomorulin in the formation and maintenance of the epithelial junctional complex. *J. Cell Biol.* 107:1575–1587.

Hall, P. A., P. J. Coates, B. Ansari, and D. Hopwood. 1994. Regulation of cell number in mammalian gastrointestinal tract: the importance of apoptosis. *J. Cell Sci.* 107:3569–3577.

Hermiston, M. L., C. B. Latham, J. I. Gordon, and K. A. Roth. 1992. Simultaneous localization of six antigens in single sections of transgenic mouse intestine using a combination of light and fluorescence microscopy. *J. Histochem. Cytochem.* 40:1283–1290.

Hermiston, M. L., R. P. Green, and J. I. Gordon. 1993. Chimeric- transgenic mice represent a powerful tool for studying how the proliferation and differentiation programs of intestinal epithelial cell lineages are regulated. *Proc. Natl. Acad. Sci. USA.* 90:8866–8870.

Hermiston, M. L., T. C. Simon, M. W. Crossman, and J. I. Gordon. 1994. Model systems for studying cell fate specification and differentiation in the gut epithelium. *In* Physiology of the Gastrointestinal Tract. Third Edition. L. R. Johnson, editor. Raven Press, New York. pp. 521–569.

Hinck, L., I. S. Näthke, J. Papkoff, and W. J. Nelson. 1994. Dynamics of cadherin/catenin complex formation: novel protein interactions and pathways of complex assembly. *J. Cell Biol.* 125:1327–1340.

Hodivala, K. J., and F. M. Watt. 1994. Evidence that cadherins play a role in the down regulation of integrin expression that occurs during keratinocyte terminal differentiation. *J. Cell Biol.* 124:589–600.

Holt, C. E., P. Lemaire, and J. B. Gurdon. 1994. Cadherin-mediated cell interactions are necessary for the activation of MyoD in *Xenopus* mesoderm. *Proc. Natl. Acad. Sci. USA.* 91:10844–10848.

Hülsken, J., J. Behrens, and W. Birchmeier. 1994. Tumor-suppressor gene products in cell contacts: the cadherin-APC-*armadillo* connection. *Curr. Opin. Cell Biol.* 6:711–716.

Itzkowitz, S. H., M. Yuan, C. K. Montgomery, T. Kjeldsen, H. K. Takahashi, W. L. Bigbee, and Y. S. Kim. 1989. Expression of Tn, sialosyl Tn, and T antigens in human colon cancer. *Cancer Res.* 49:197–204.

Jinguji, Y., and H. Ishikawa. 1992. Electron microscopic observations on the maintenance of the tight junction during cell division in the epithelium of the mouse small intestine. *Cell Struct. Func.* 17:27–37.

Jongen, W. M. F., D. J. Fitzgerald, M. Asamoto, C. Piccoli, T. J. Slaga, D. Gros, M. Takeichi, and H. Yamasaki. 1991. Regulation of connexin 43-mediated gap junctional intercellular communication by Ca^{2+} in mouse epidermal cells is controlled by E-cadherin. *J. Cell Biol.* 114:545–555.

Kemler, R. 1992. Classical cadherins. *Sem. Cell Biol.* 3:149–155.

Kemler, R. 1993. From cadherins to catenins: cytoplasmic protein interactions and regulation of cell adhesion. *Trends Genet.* 9:317–321.

Kim, S. H., K. A. Roth, A. R. Moser, and J. I. Gordon. 1993. Transgenic mouse models that explore the multistep hypothesis of intestinal neoplasia. *J. Cell Biol.* 123:877–893.

Kim, S. H., K. A. Roth, C. G. Coopersmith, J. M. Pipas, and J. I. Gordon. 1994. Expression of wild type and mutant Simian virus 40 large tumor antigens in villus-associated enterocytes of transgenic mice. *Proc. Natl. Acad. Sci. USA.* 91:6914–6918.

Kinter, C. 1992. Regulation of embryonic cell adhesion by the cadherin cytoplasmic domain. *Cell.* 69:225–236.

Kolber, M. A., K. O. Broschat, and B. Landa-Gonzalez. 1990. Cytochalasin B induces cellular DNA fragmentation. *FASEB (Fed. Am. Soc. Exp. Biol.) J.* 4:3021–3027.

Larue, L., M. Ohsugi, J. Hirchenhain, and R. Kemler. 1994. E-cadherin null mutant embryos fail to form a trophectoderm epithelium. *Proc. Natl. Acad. Sci. USA.* 91:8263–8267.

Levine, E., C. H. Lee, C. Kintner, and B. M. Gumbiner. 1994. Selective disruption of E-cadherin function in early *Xenopus* embryos by a dominant negative mutant. *Development.* 120:901–909.

Lo, D. 1992. T cell tolerance. *Curr. Opin. Immunol.* 4:711–715.

Loeffler, M., A. Birke, D. Winton, and C. Potten. 1993. Somatic mutation, monoclonality, and stochastic models of stem cell organization in the intestinal crypt. *J. Theor. Biol.* 160:471–491.

Madara, J. L. 1990. Maintenance of the macromolecular barrier at cell extrusion sites in intestinal epithelium: physiological rearrangement of tight junctions. *J. Memb. Biol.* 116:177–184.

McCrea, P., W. M. Brieher, and B. M. Gumbiner. 1993. Induction of a secondary body axis in *Xenopus* embryos by antibodies to β-catenin. *J. Cell Biol.* 123:477–485.

McNeill, H., M. Ozawa, R. Kemler, and W. J. Nelson. 1990. Novel function of the cell adhesion moelcule uvomorulin as an inducer of cell surface polarity. *Cell.* 62:309–316.

Meredith, J. E., B. Fazeli, and M. A. Schwartz. 1993. The extracellular matrix as a cell survival factor. *Mol. Biol. Cell.* 4:953–961.

Montgomery, A. M. P., R. A. Reisfeld, and D. A. Cheresh. 1994. Integrin $\alpha_v\beta_3$ rescues melanoma cells from apoptosis in three-dimensional dermal collagen. *Proc. Natl. Acad. Sci. USA.* 91:8856–8860.

Moser, A. R., H. C. Pitot, and W. F. Dove. 1990. A dominant mutation that predisposes to multiple intestinal neoplasia in the mouse. *Science (Wash. DC).* 247:322–324.

Moser, A. R., W. F. Dove, K. A. Roth, and J. I. Gordon. 1992. The *Min* (multiple intestinal neoplasia) mutation: its effect on gut epithelial cell differentiation and interaction with a modifier system. *J. Cell Biol.* 116:1517–1526.

Nagafuchi, A., and M. Takeichi. 1988. Transmembrane control of cadherin-mediated cell adhesion: a 94kDa protein functionally associated with a specific region of the cytoplasmic domain of E-cadherin. *Cell Regulation.* 1:37–44.

Nagafuchi, A., Y. Schirayoshi, K. Okazaki, K. Yasuda, and M. Takeichi. 1987. Transformation of cell adhesion properties by exogenously introduced E-cadherin cDNA. *Nature (Lond.).* 329:340–343.

Näthke, I. S., L. Hinck, J. R. Swedlow, J. Papkoff, and W. J. Nelson. 1994. Defining interactions and distributions of cadherin and catenin complexes in polarized epithelial cells. *J. Cell Biol.* 125:1341–1352.

Ozawa, M., H. Baribault, and R. Kemler. 1989. The cytoplasmic domain of the cell adhesion molecule uvomorulin associates with three independent proteins structurally related in different species. *EMBO (Eur. Mol. Biol. Organ.) J.* 8:1711–1717.

Ozawa, M., M. Ringwald, and R. Kemler. 1990. Uvomorulin-catenin complex formation is regulated by a specific domain in the cytoplasmic region of the cell adhesion molecule. *Proc. Natl. Acad. Sci. USA.* 87:4246–4250.

Peifer, M., S. Orsulic, D. Sweeton, and E. Wieschaus. 1993. A role for the *Drosophila* segment polarity gene *armadillo* in cell adhesion and cytoskeletal integrity during oogenesis. *Development.* 118:1191–1207.

Raff, M. C. 1992. Social controls on cell survival and cell death. *Nature (Lond.).* 356:397–399.

Ranscht, B. 1994. Cadherins and catenins: interactions and functions in embryonic development. *Curr. Opin. Cell Biol.* 6:740–746.

Re, F., A. Zanetti, M. Sironi, N. Polentarutti, L. Lanfrancone, E. Dejana, and F. Colotta. 1994. Inhibition of anchorage-dependent cell spreading triggers apoptosis in cultured human endothelial cells. *J. Cell Biol.* 127:537–546.

Robertson, E. J. 1987. Embryo-derived stem cell lines. *In* Teratocarcinomas and Embryonic Stem Cells: a Practical Approach. E. J. Robertson, editor. IRL Press, Oxford. pp. 71–112.

Roth, K. A., J. W. Hertz, and J. I. Gordon. 1990. Mapping enteroendocrine cell populations in transgenic mice reveals an unexpected degree of complexity in cellular differentiation within the gastrointestinal tract. *J. Cell Biol.* 110:1791–1801.

Rubinfeld, B., B. Souza, I. Albert, O. Müller, S. H. Chamberlain, F. R. Masiarz, S. Munemitsu, and P. Polakis. 1993. Association of the APC gene product with β-catenin. *Science (Wash. DC).* 262:1731–1734.

Ruoslahti, E., and J. C. Reed. 1994. Anchorage dependence, integrins, and apoptosis. *Cell.* 7:477–478.

Sansonetti, P. J., J. Mounier, M. C. Prévost, and R.-M. Mège. 1994. Cadherin expression is required for the spread of *Shigella flexneri* between epithelial cells. *Cell.* 76:829–839.

Schmidt, G. H., M. M. Wilkinson, and B. A. J. Ponder. 1985. Cell migration pathway in the intestinal epithelium: an *in situ* marker system using mouse aggregation chimeras. *Cell.* 40:425–429.

Schmidt, G. H., D. J. Winton, and B. A. J. Ponder. 1988. Development of the pattern of cell renewal in the crypt-*villus* unit of chimaeric mouse small intestine. *Development.* 103:785–790.

Schmidt, J. W., P. A. Piepenhagen, and W. J. Nelson. 1993. Modulation of epithelial morphogenesis and cell fate by cell-to-cell signals and regulated cell adhesion. *Sem. Cell Biol.* 4:161–173.

Simon, T. C., K. A. Roth, and J. I. Gordon. 1993. Use of transgenic mice to map *cis*-acting elements in the liver fatty acid binding protein gene (*Fabpl*) that regulate its cell lineage-specific, differentiation-dependent and spatial patterns of expression in the intestinal epithelium and in the liver acinus. *J. Biol. Chem.* 268:18345–18358.

Simonet, W. S., T. M. Hughes, H. Q. Nguyen, L. D. Trebasky, D. M. Danilenko, and E. S. Medlock. 1994. Long-term impaired neutrophil migration in mice overexpressing human interleukin 8. *J. Clin. Invest.* 94:1310–1319.

Smith, K. J., K. A. Johnson, T. M. Bryan, D. E. Hill, S. Markowitz, J. K. V. Willson, C. Paraskeva, G. M. Peterson, S. R. Hamilton, B. Vogelstein, et

al. 1993. The APC gene product in normal and tumor cells. *Proc. Natl. Acad. Sci. USA.* 90:2846–2850.

Su, L.-K., B. Kinzler, B. Vogelstein, A. C. Preisinger, A. R. Moser, C. Luongo, K. A. Gould, and W. F. Dove. 1992. Multiple intenstinal neoplasia caused by a mutation in the murine homolog of the APC gene. *Science (Wash. DC).* 256:668–670.

Su, L.-K., B. Vogelstein, and K. W. Kinzler. 1993. Association of the APC tumor suppressor protein with catenins. *Science (Wash. DC).* 262:1734–1737.

Sweetser, D. A., E. H. Birkenmeier, P. C. Hoppe, D. W. McKeel, and J. I. Gordon. 1988. Mechanisms underlying generation of gradients in gene expression within the intestine: an analysis using transgenic mice containing fatty acid binding protein/human growth hormone fusion genes. *Genes & Dev.* 2:1318–1332.

Takeichi, M. 1988. The cadherins: cell-cell adhesion molecules controlling animal morphogenesis. *Development.* 102:639–655.

Takeichi, M. 1991. Cadherin cell adhesion receptors as a morphogenetic regulator. *Science (Wash. DC).* 251:1451–1455.

Takeichi, M. 1993. Cadherins in cancer: implications for invasion and metastasis. *Curr. Opin. Cell Biol.* 5:806–811.

Tybulewicz, V. L. J., C. E. Crawford, P. K. Jackson, R. T. Bronson, and R. C. Mulligan. 1991. Neonatal lethality and lymphopenia in mice with a homozygous disruption of the c-*abl* protooncogene. *Cell.* 65:1153–1163.

Vestweber, D., and R. Kemler. 1985. Identification of a putative cell adhesion domain of uvomorulin. *EMBO (Eur. Mol. Biol. Organ.) J.* 4:3393–3398.

Vleminckx, K., L. Vakaet, Jr., M. Mareel, W. Fiers, and F. Van Roy. 1991. Genetic manipulation of E-cadherin expression by epithelial tumor cells reveals an invasion suppressor role. *Cell.* 66:107–119.

Walker, R. I., I. Brook, J. W. Costerton, T. MacVittie, and M. L. Myhal. 1985. Possible association of mucous blanket integrity with postirradiation colonization resistance. *Radiat. Res.* 104:346–357.

Watabe, M., A. Nagafuchi, S. Tsukita, and M. Takeichi. 1994. Induction of polarized cell-cell association and retardation of growth by activation of the E-cadherin-catenin adhesion system in a dispersed carcinoma line. *J. Cell Biol.* 127:247–256.

Weiser, M. M., J. R. F. Walters, and J. R. Wilson. 1986. Intestinal cell membranes. *Int. Rev. Cytol.* 101:1–57.

Wheelock, M. J., and P. J. Jensen. 1992. Regulation of keratinocyte intercellular junction organization and epidermal morphogenesis by E-cadherin. *J. Cell Biol.* 117:415–425.

Wright, N. A., and M. Irwin. 1982. The kinetics of villus cells populations in the mouse small intestine: normal villus–the steady state requirement. *Cell Tissue Kinet.* 15:595–609.

Wyllie, A. H., J. F. R. Kerr, and A. R. Currie. 1980. Cell death: the significance of apoptosis. *Int. Rev. Cytol.* 68:251–305.

Zhou, L., C. R. Dey, S. E. Wert, M. D. DuVall, R. A. Frizzell, and J. A. Whitsett. 1994. Correction of lethal intestinal defect in a mouse model of cystic fibrosis by human *CFTR*. *Science (Wash. DC).* 266:1705–1708.